PLASMA SPRAYING

Motto: *„Plasma spraying is not a science but rather an ART“*
Prof. Herbert HERMAN, SUNY, USA

1. **Introduction: “What is plasma spraying and why it is useful to develop the plasma spraying technology?”**
2. **Methods that are applied for deposition of plasma-sprayed coatings.**
3. **Conditions for creation of good-quality plasma-sprayed coatings and free-standing parts.**
4. **Comments to the structure of plasma-sprayed coatings.**
5. **Comments to phase composition of plasma-sprayed coatings.**
6. **Examples of applications of plasma spraying.**
7. **Conclusion, future prospects.**

All displayed materials are courtesy of the Institute of Plasma Physics Academy of Sciences of the Czech Republic. Marked slides are property of the State University of New York at Stony Brook, U.S.A.

IPP INSTITUTE OF PLASMA PHYSICS
ACADEMY OF SCIENCES OF THE CZECH REPUBLIC

SUNY
THE STATE UNIVERSITY of NEW YORK

1. INTRODUCTION – a few dates from the history of TS

- well known figure illustrating development of TS omits high throughput systems based on liquid (water) stabilization

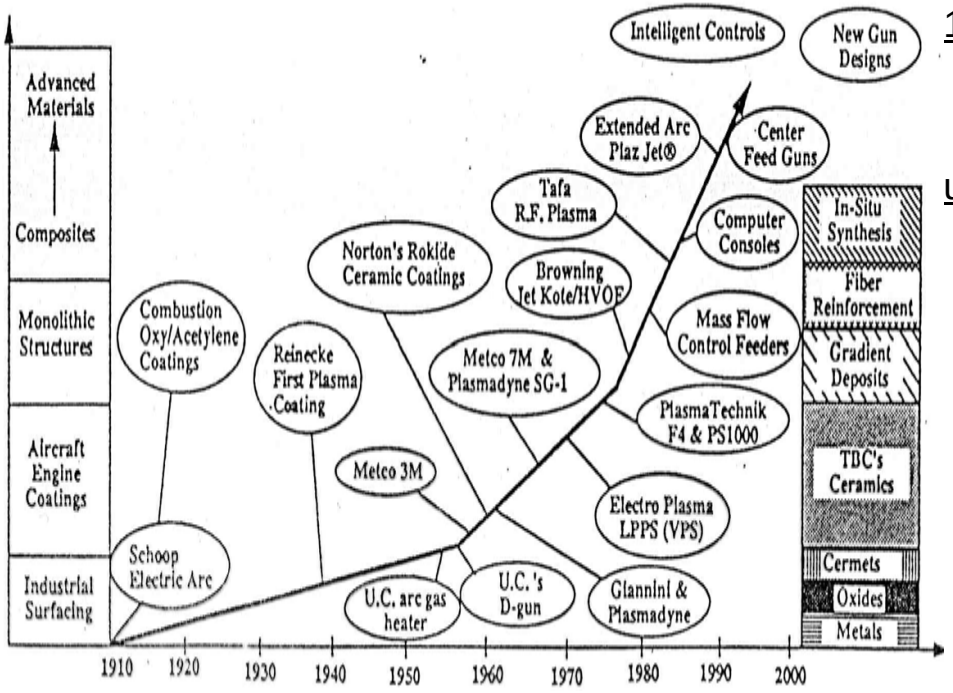

1922: Siemens (H. Gerdien, A. Lotz) principle of the liquid stabilization (LP)

1934: basic principle of plasma spraying

1962: Prague (V. Veselý, T. Kugler) first use of LP (WSP) for plasma spraying

up to now:

- several different technical designs reported (Alusuiss, Novosibirsk, …)
- a larger commercial distribution reached only by CS PAL 160 with several tens of units (80's) followed by WSP® 500 at the end of 90's

Energy contained in a plasma

At otherwise comparable conditions exceeds the energy contained in a plasma the energy contained in an ideal gas considerably. Apart from that is for plasma typical the distribution of energy into several particular components (energy stacks, energetic degrees of freedom) that mutually interact. The energy components contained in a plasma are as follows:

- energy of the electric field
- energy of the magnetic field
- ionization energy
- translational energy of neutral and charged particles
- excitation energy (electronic excitation, energy of vibrations and rotations of molecules/molecular ions)
- energy of the radiation
- energy of collective effects in a plasma (oscillations, waves)

The number and magnitude of the mentioned energy components depends on conditions in which the plasma exists. Generally, they do not have to be in thermal equilibrium, i.e. they cannot be generally described by a common temperature.

Enthalpy of plasma

For technical use of plasma as a media carrying energy in a stationary working process, e.g. in plasma spraying, is at a constant pressure p very important the notion of specific enthalpy h of plasma, $h = u + pv$, where u stands for internal energy. This physical quantity namely directly explains the energy flux, e.g. at the heating of materials using plasma.

In a gas that has f degrees of freedom holds for every particle (related to the unit of mass): internal energy $u = fkT/2m$, $pV=kT/m$. By easy manipulation we obtain for $h = (f + 2)\, kT/2m$. The course of the increase of plasma enthalpy with temperature is non-linear. That is due to the fact that at higher temperatures contribute to plasma enthalpy additional energy components, e.g. due to excitation, dissociation and ionization. The increase of the enthalpy formally means the increase of the number of degrees (quasi-degrees) of freedom.

In figure we see the enthalpy increase for H_2 a N_2. In the region of high temperatures gains the enthalpy by order of magnitude greater value compared to that of ideal gas. Especially marked differences we find in the course of the specific heat capacity $c_p = \left(\frac{\partial h}{\partial T}\right)_p$.

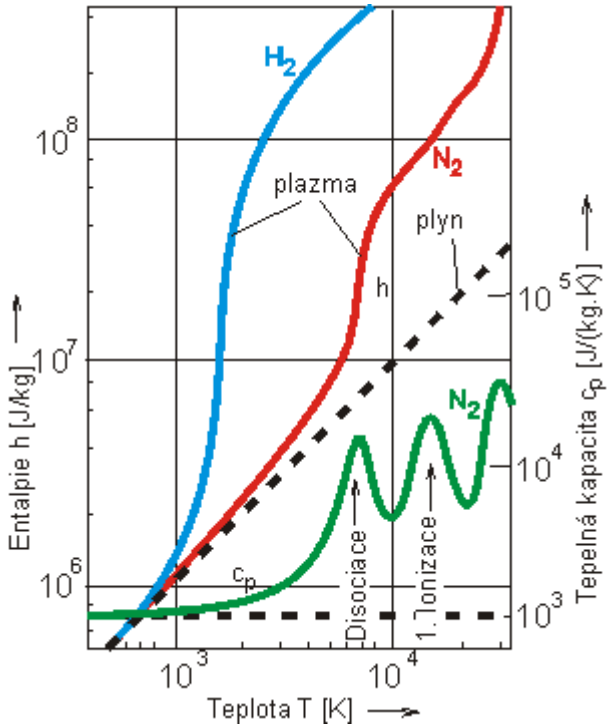

Enthalpy h of H_2 and *N_2 plasma and the specific heat capacity c_p of N_2 plasma, as a function of temperature T at atmospheric pressure. It is seen that H_2 is very good energy carrier. Dashed lines represent values for ideal gas.*

While for the ideal gas holds that $c_p = (f + 2)kT/2m = konst.$, has the plot of the the specific heat capacity for plasma non-monotonous course with several maxima at the regions of dissociation, 1. ionization, 2. ionization etc. At higher temperature the plasma can then have 100 and more quasi-degrees of freedom. Despite of that the volume energy density is small, around 1 J/cm^3, which is due to the small particle density. On the other hand in order to keep this energy density it is necessary to supply large **power** density, e.g. 1 kW/cm^3. That is due to the inverse volume processes (e.g. de-excitation, recombination, association), by means of which is the energy from plasma continuously radiated out. If the plasma is in contact with a wall, e.g. with the surface of the sprayed powder, then the wall is heated due to similar processes. Plasma burners are thus possible to be applied for cutting, welding and melting of materials. In plasma spraying they are used for deposition of layers and manufacturing free standing parts from materials that are otherwise difficult to melt, e.g. refractory metals, different ceramics etc.

Plasma spray: taming a complex process

All thermal-spray processes use a device (the gun) to melt and propel a coating material at high velocities onto a substrate where solidification occurs rapidly (with rate of the order million degrees per second), forming either a protective coating or a bulk shape. There are basically three types of thermal spray guns: plasma, combustion-flame, and two-wire electric arc. The consumable coating material (feedstock) is in the form of powder, wire, or rod, and combustion or electrical power supplies the energy to achieve melting and acceleration.

Plasma-arc spraying uses a thermal plasma (the highest temperature heat source), and is the most versatile thermal-spraying process. The thermal plasma, a dense, highly ionized gas, has a sufficiently high enthalpy density to melt and deposit powders of virtually any metal alloy or refractory ceramic, as well as combinations of materials.

Traditional DC thermal-plasma units can spray powders at high velocities (>200 m/sec), yielding good coating densities, potentially approaching theoretical density. Plasma spraying results in fine, essentially equiaxed grains, without extensive columnar boundaries, of particular advantage in certain ceramics applications (thermal-barrier coatings, for example). Coatings are chemically homogeneous; there is no (or controllable) change in composition with thickness. It is possible, however, to change from depositing a metal, to a continuously varying metal-ceramic mixture, to a ceramic-rich mixture, and finally to a completely ceramic outer layer, using programmed automation without intermediate delays in spraying or in part handling.

Off-the-shelf plasma-spray equipment offers the capability of high coating-feedstock throughput (3 kg/hr), and special high-power guns can achieve a feedstock (e.g., alumina) throughput of over 25 kg/hr. Aside from normally spraying in air, it is possible, and sometimes essential, to plasma spray in a reduced-pressure environment chamber. Underwater spraying also is possible.

The plasma flame is maintained by a steady, continuous-arc discharge of flowing inert gas, generally argon plus a small percentage of an enthalpy-enhancing diatomic gas, such as hydrogen. Feedstock powder (10 to 70 μm diameter) is carried by an inert gas into the emerging plasma flame. The particles melt in transit without vaporizing excessively, are accelerated, and impinge on the substrate where they flatten and solidify at cooling rates similar to those achieved in rapid-solidification processes.

Much of the heat contained within the particles being deposited, as well as the heat of solidification and the heat of the plasma flame, is removed by conduction through the substrate. Consequently, precautions must be taken to prevent thermal degradation of substrate properties, or to prevent a metal substrate and/or coating from becoming excessively oxidized. Both the substrate and coating contract upon cooling, which can generate high residual stresses if a significant difference in coefficients of thermal expansion exists; these stresses can lead to coating delamination.

While there are hundreds of parameters that influence the plasma-arc spraying process, about 12 have been identified as having the strongest influence on coating properties and the survivability of the coating system. Improved control of these parameters was the focus of many developments that have occurred during the past few years, and is the focus of many current developments. These include incorporating empirical or real-time feedback looping, redesigning fundamental gun components and feedstock powders (e.g. chemical composition, size distribution, and shape), and rethinking power-supply design.

There also have been major changes in gas-handling equipment. Mass-flow control and metering are replacing traditional analog gages, which enable digital output with feedback potential. Powder feeders also have changed, with fluidized-bed feeders becoming common; these feeders permit smooth flow (less pulsing) of a wider range of powder types.

THREE TYPES OF POWDER FEEDERS

Pressurized volumetric powder feeder

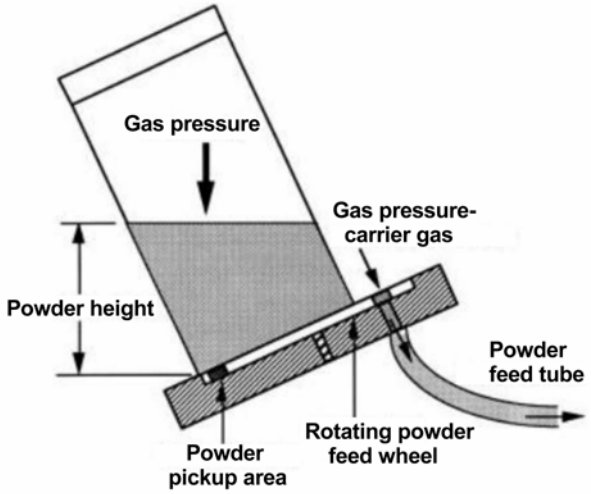

Aspirating volumetric powder feeder

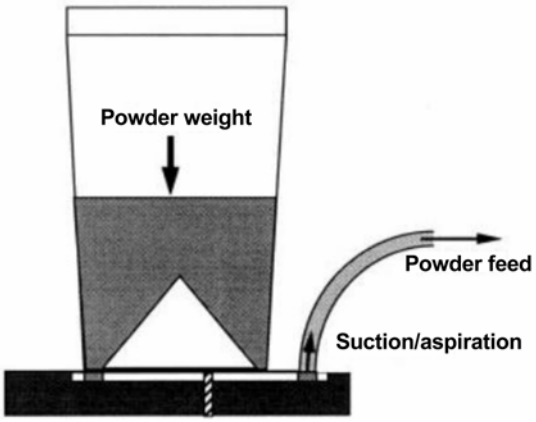

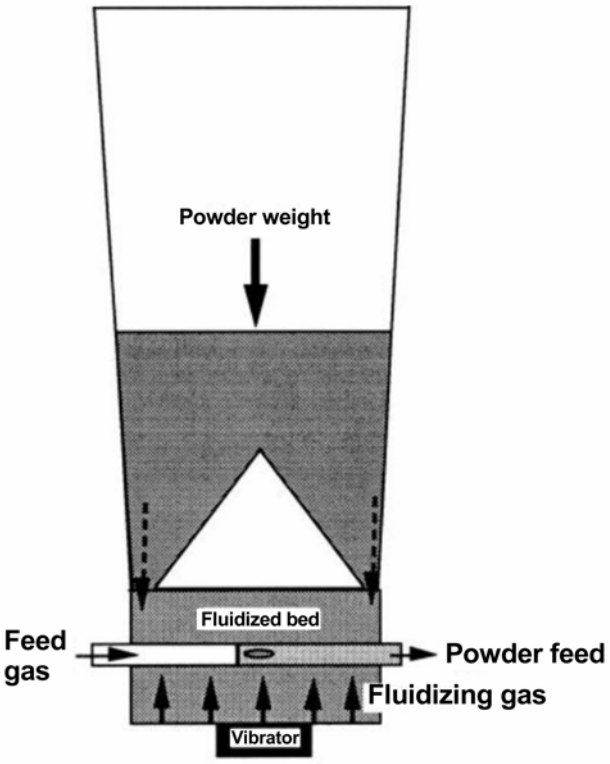

Fluidized-bed powder feeder

Combustion-flame spraying generally uses an oxyacetylene flame to melt and spray either powder or wire feedstock. Due to its lower flame temperature and particle velocity compared with plasma spraying, flame spraying produces a less dense coating having lower adhesion strength. However, flame spraying is simpler in principle and operation, and system and production costs are lower than for plasma spraying. An additional consideration is the possible use of less-skilled operators because the process is more forgiving.

The hypervelocity oxyfuel (**HVOF**) gun represents a major development in thermal-spray technology. HVOF guns burn oxygen and fuel and carry the combustion products through a nozzle with subsequent free expansion. This arrangement results in hypersonic flame gas velocities, and by introducing the feedstock powder "up-wind", powder particles attain high heat and supersonic velocities, this permits particle flattening upon striking the substrate, thus forming a dense coating.

Two-wire, electric-arc spraying represents an important method to achieve low-cost application of metallic coatings. Most welding wires can be electric-arc sprayed at high throughput (from 30 to 50 kg/hr). During the process, two consumable wires, through which an electric current is passed, form an electric arc at the point where they intersect. The arc melts the wires and the molten metal is atomized by a continuous flow of either high-velocity compressed air or nonoxidizing gases, such as carbon dioxide, nitrogen, or argon.

PRINCIPLES OF THERMAL PLASMA SPRAYING

Principles of arc stabilization

Gas-stabilized arc

- Gas flows along the arc in the nozzle
- Usually gas flow has vortex component for better stabilization and for anode spot movement
- Anode created by exit nozzle or transferred arcs
- Power level: 1 kW – 10 MW
- Plasma temperatures: 6 000 – 20 000 K

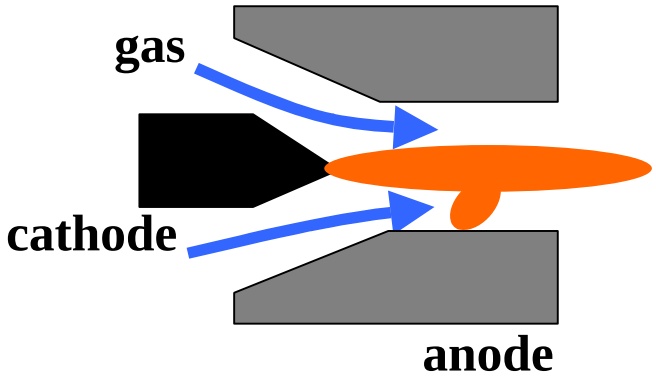

Liquid-stabilized (Gerdien) arc

- Liquid vortex is created in cylindrical chamber with tangential injection
- Arc is stabilized by its interaction with the vortex
- Anode is outside of arc chamber
- Power level: 10 – 200 kW
- Plasma temperatures: 8 000 – 50 000 K

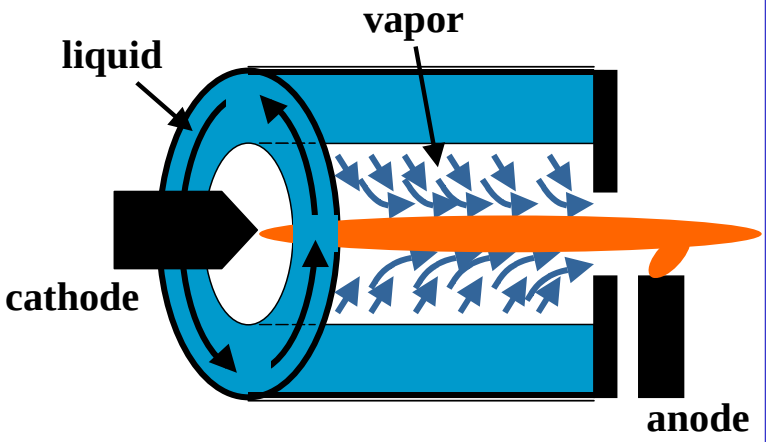

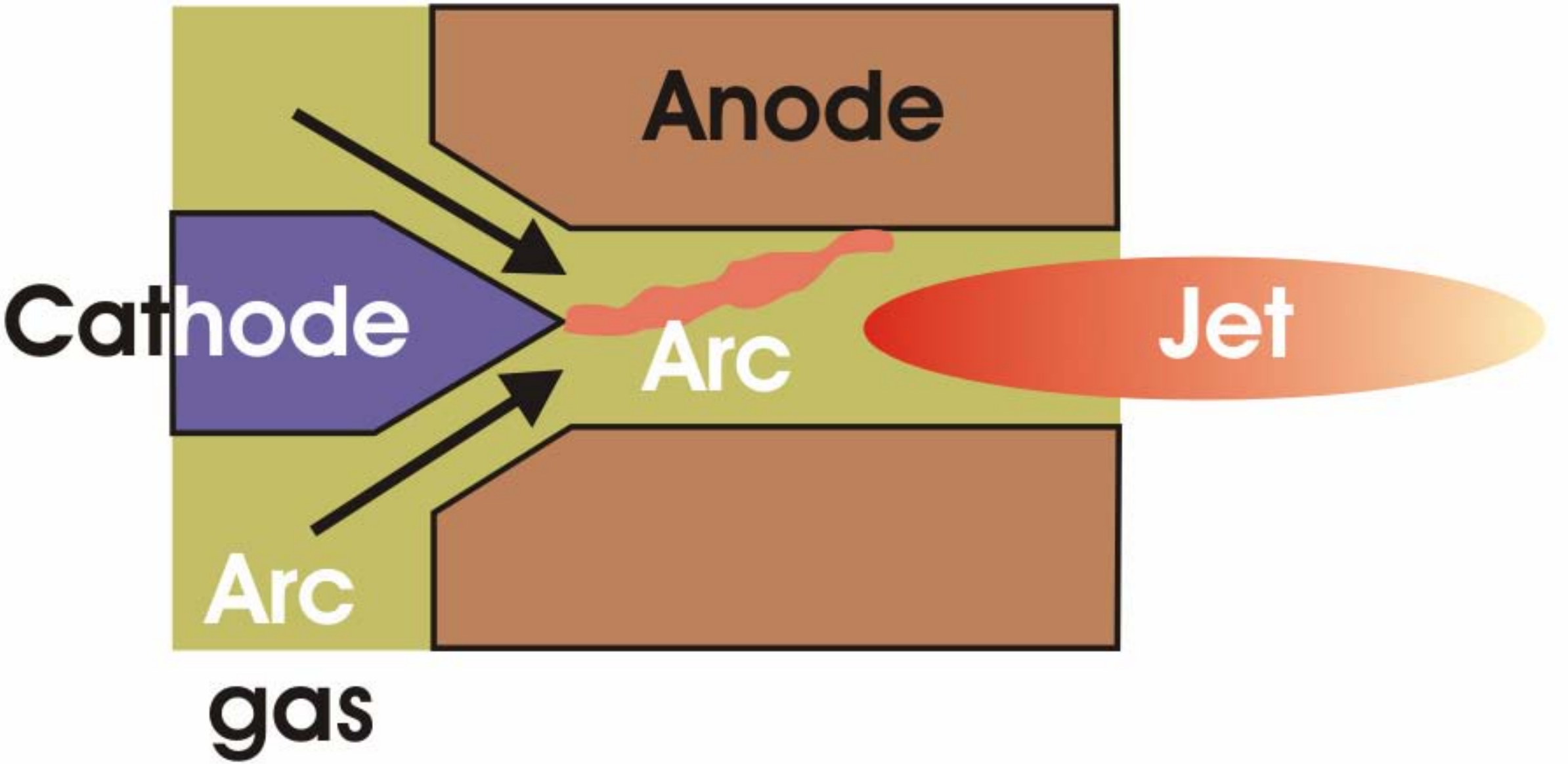
Anode
Cathode
Arc
Jet
Arc
gas

Water Stabilized Plasma Torch

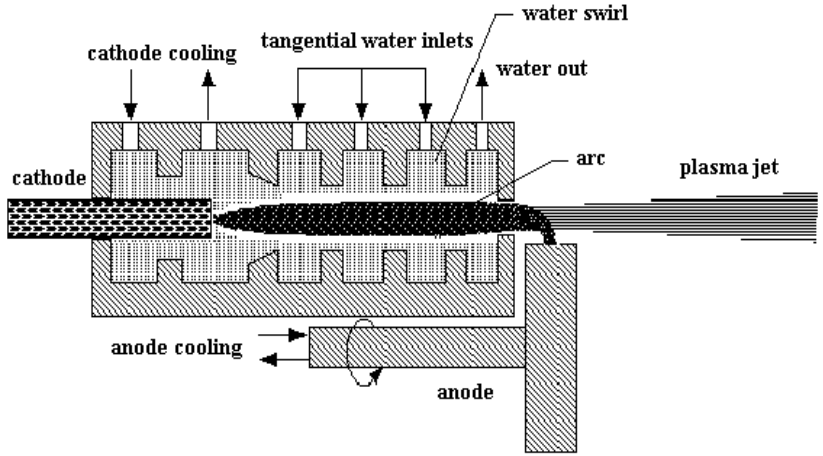

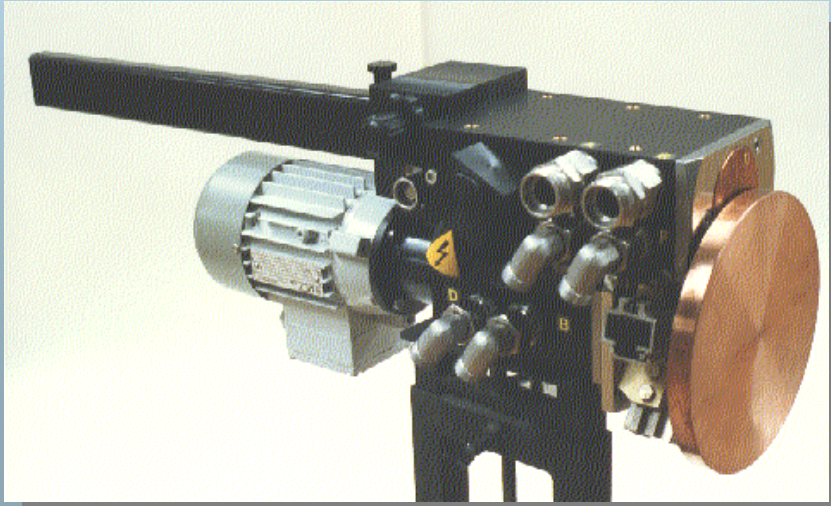

arc current: ***300 - 600 A***
arc power: ***80 - 176 kW***
arc voltage: ***267 - 293 V***

exit centerline temperature:
19 000 - 28 000 K
exit centerline velocity:
2500 - 7000 m/s
centerline plasma density:
0.9 - 2.0 g/m^{-3}

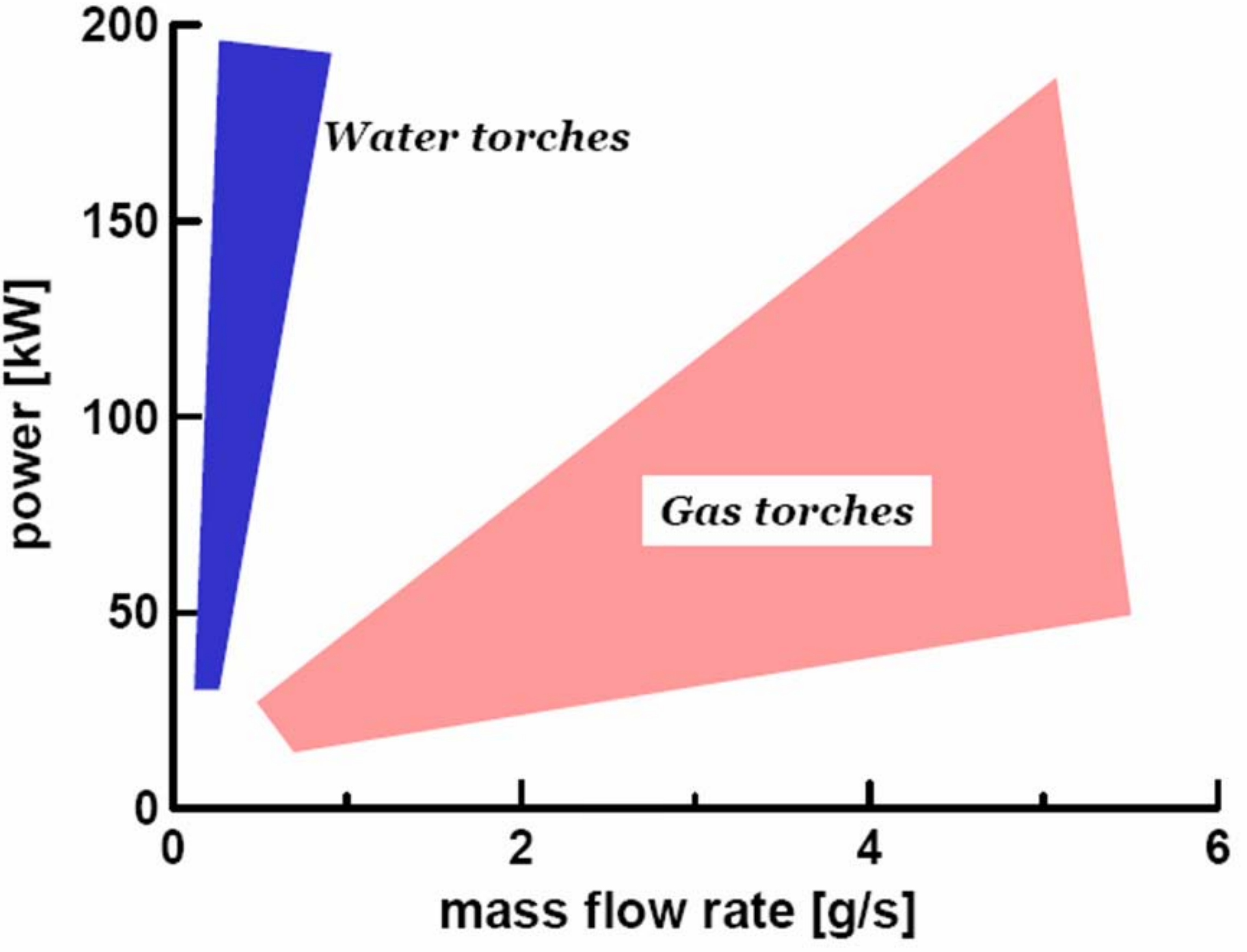
200
150
100
50
0
power [kW]
Water torches
Gas torches
0
2
4
6
mass flow rate [g/s]

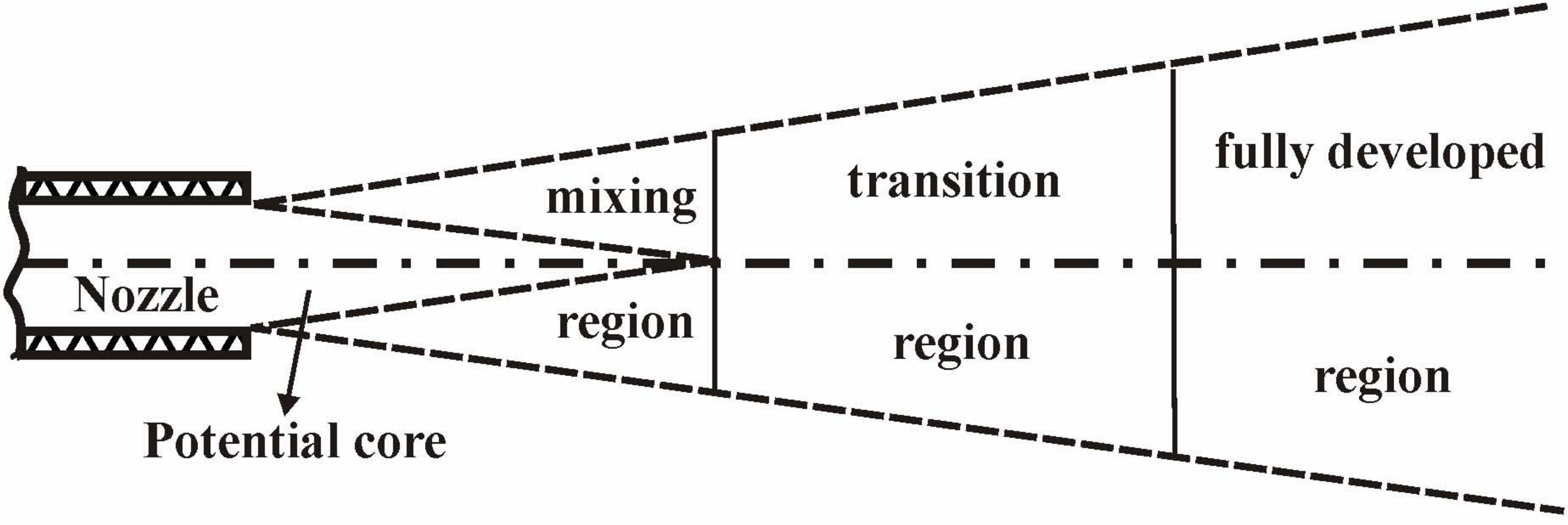
mixing
region
transition
region
fully developed
region
Nozzle
Potential core

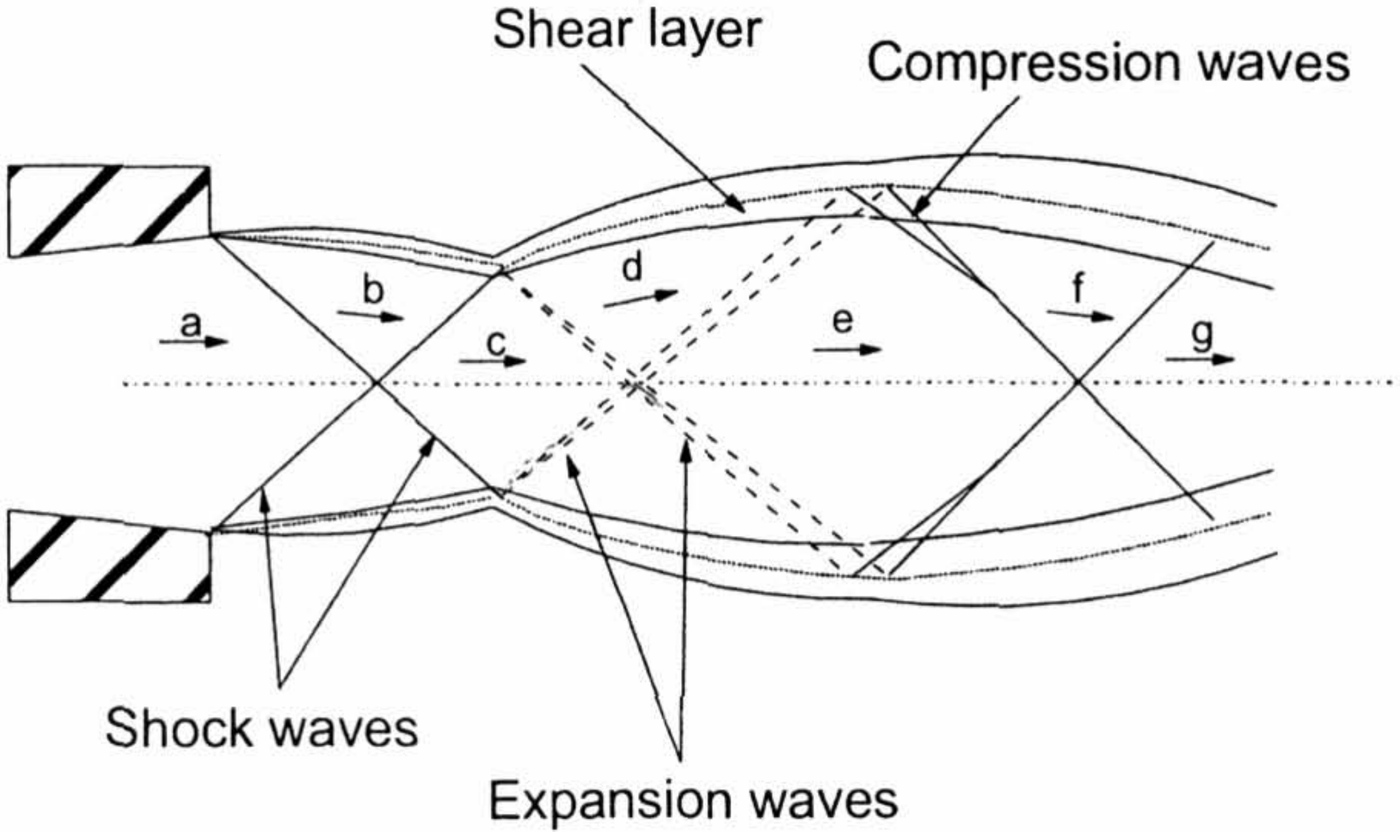
Shear layer
Compression waves
a
b
c
d
e
f
g
Shock waves
Expansion waves

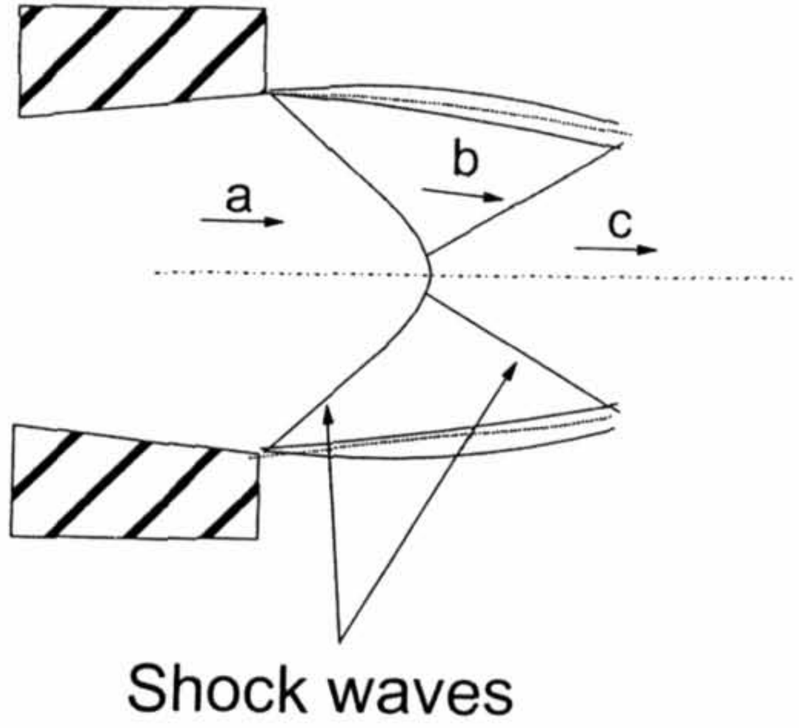
a
b
c
Shock waves

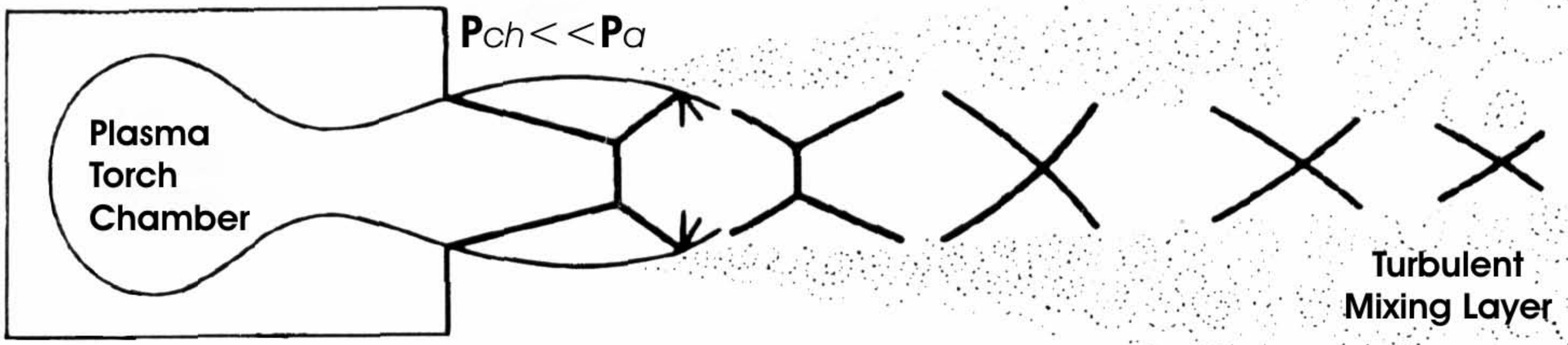
Pch<<Pa
Plasma
Torch
Chamber
Turbulent
Mixing Layer

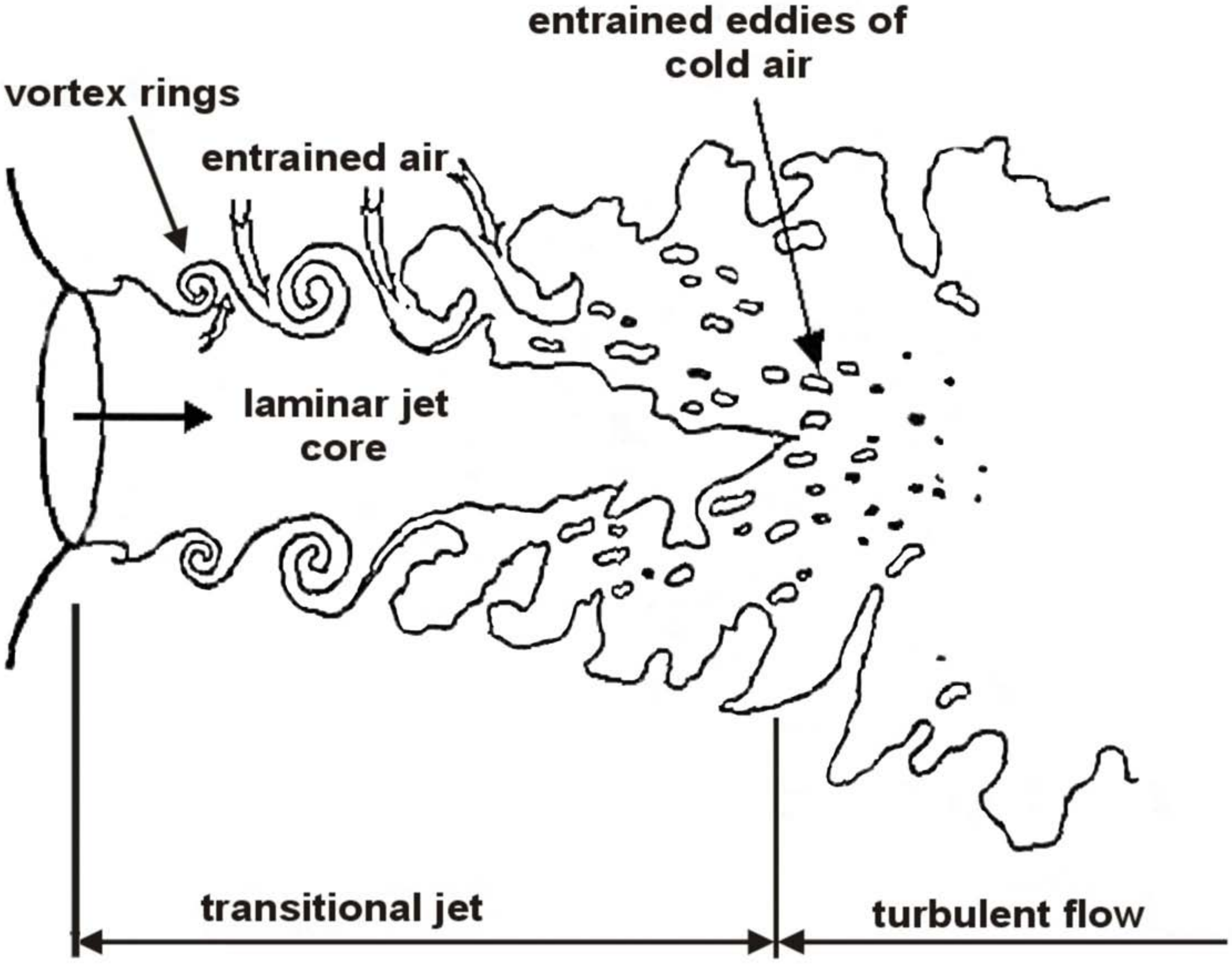
entrained eddies of
cold air
vortex rings
entrained air
laminar jet
core
transitional jet
turbulent flow

Von Kármán vortex street
in the atmosphere

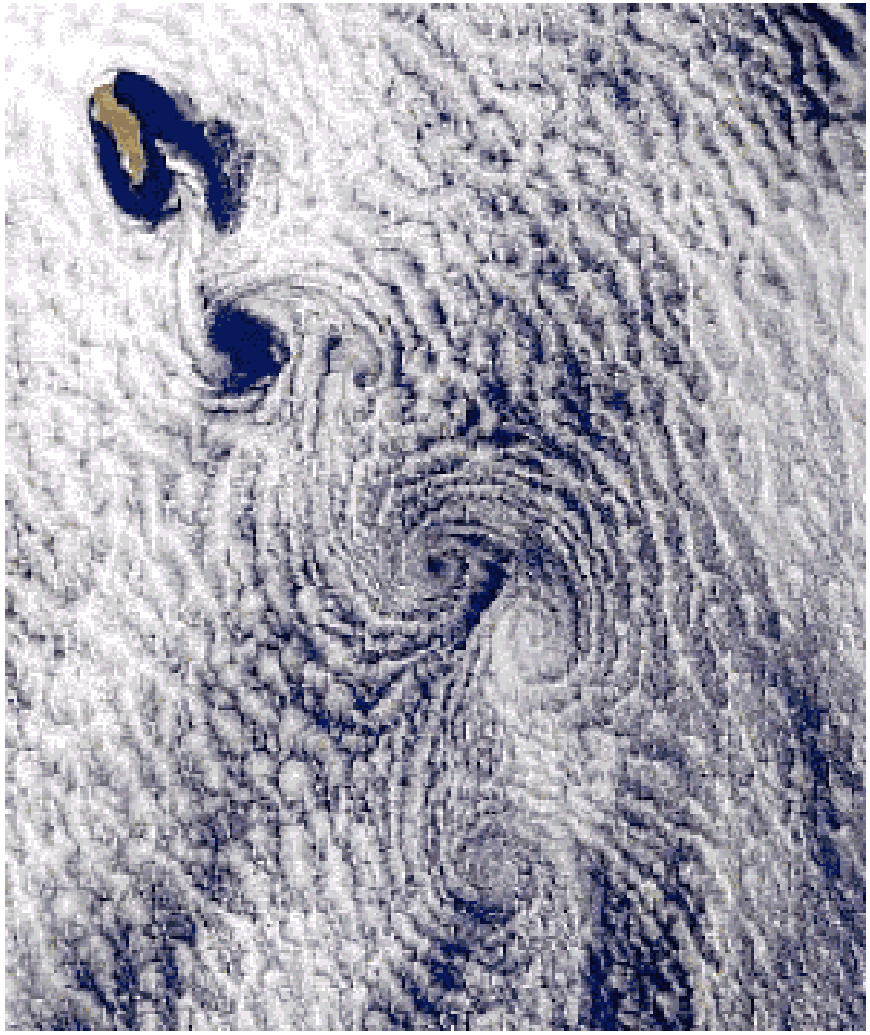

Von Kármán vortex street off the Chilean coast near the Juan Fernandez Islands.

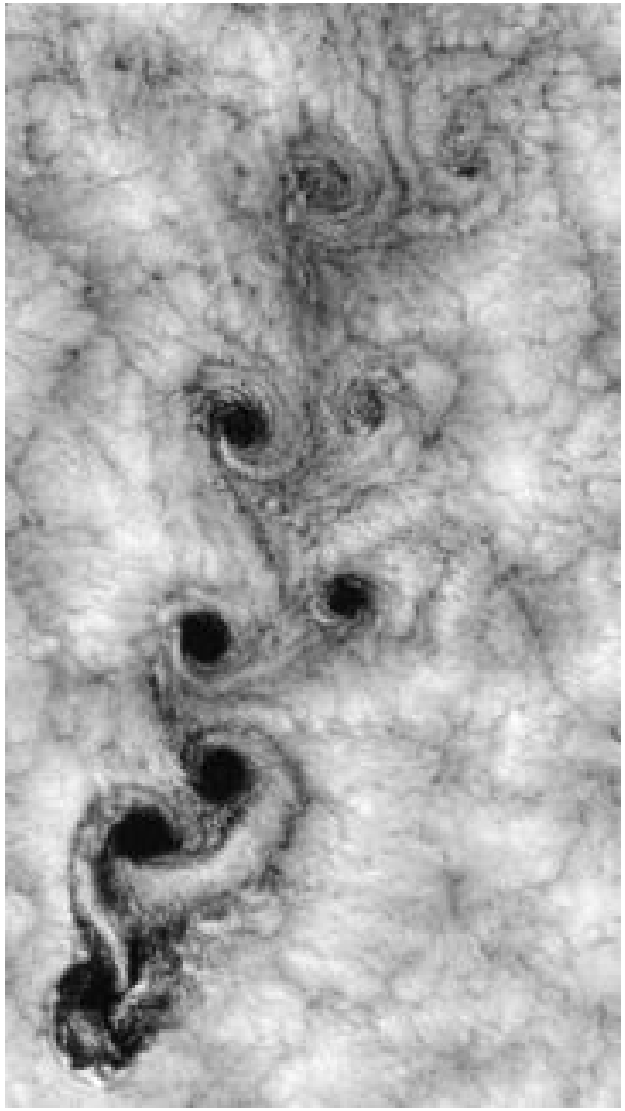

WSP at work

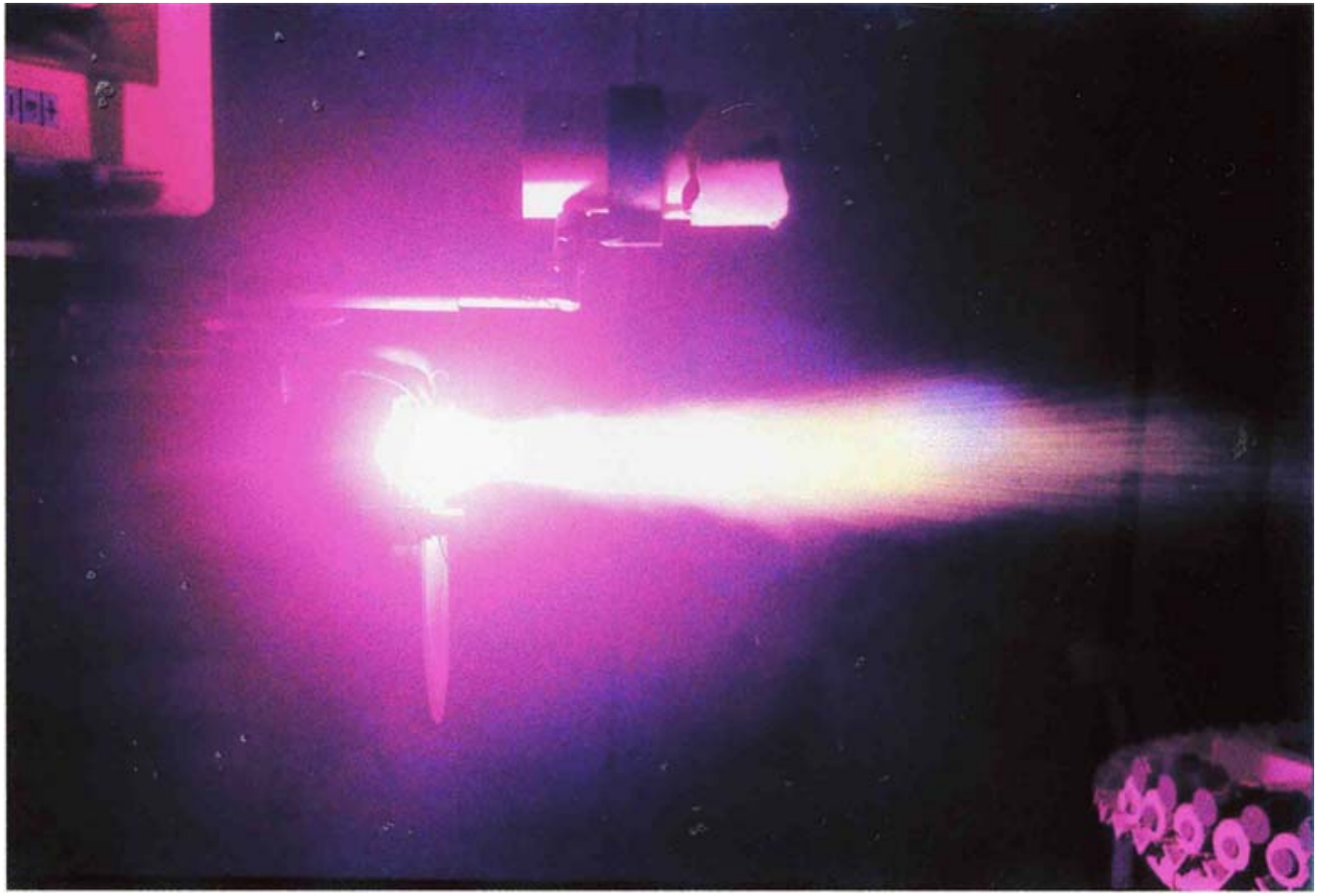

2. THERMAL SPRAYING

2.1 Methods of thermal spraying.

Definition: "A process in which molten or semi-molten particles are applied by <u>impact</u> onto a substrate".

Principle: ➔ a heat source melting feedstock +

➔ a medium accelerating molten feedstock +

➔ an activated substrate (cleaned, grit-blasted)

Common features of all thermal spray coatings:

➔ lenticular or **lamellar structure = splats**
from rapid solidification and rapid flattening of melted particles striking a cold surface at high velocities

➔ **non-equilibrium and often non-stoichiometric structures**

= ***material with special properties***

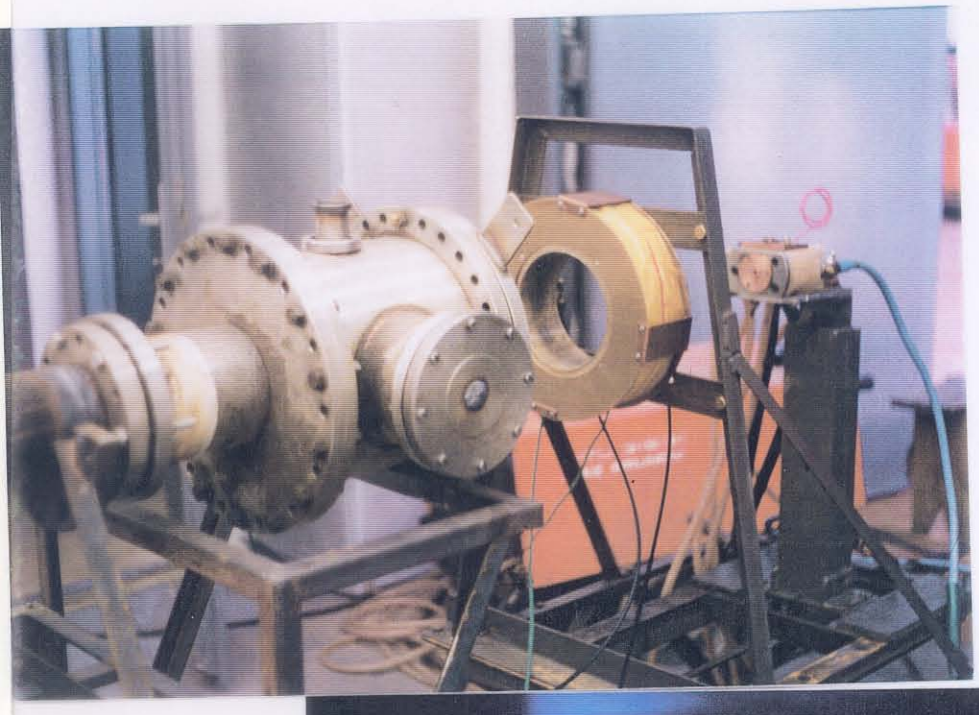

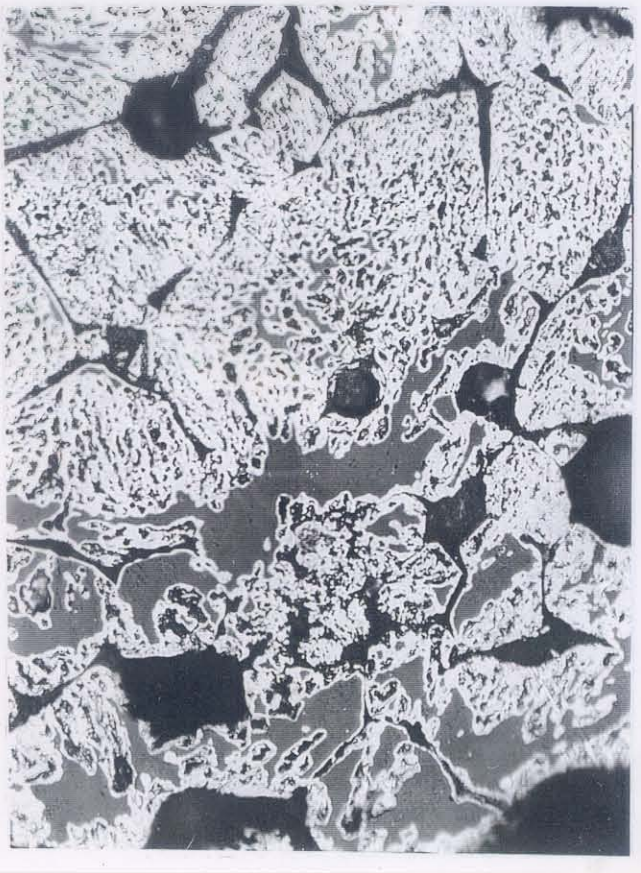

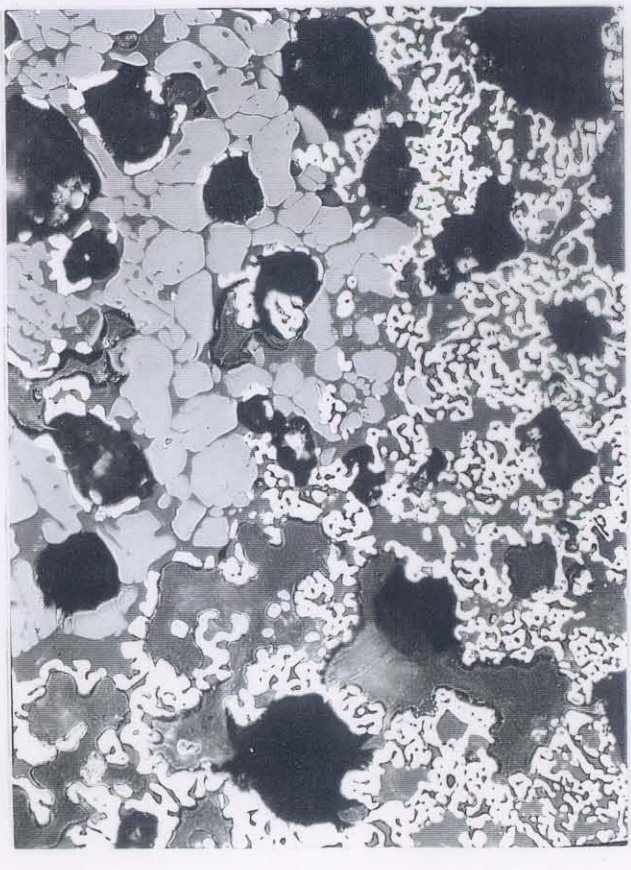

NON-EQUILIBRIUM EFFECTS DURING THERMAL SPRAY PROCESSING

Particle Flame Interaction

Oxidation
Decomposition
Volatilization

Rapid Solidification

Supersaturation
Amorphization
Metastable phases

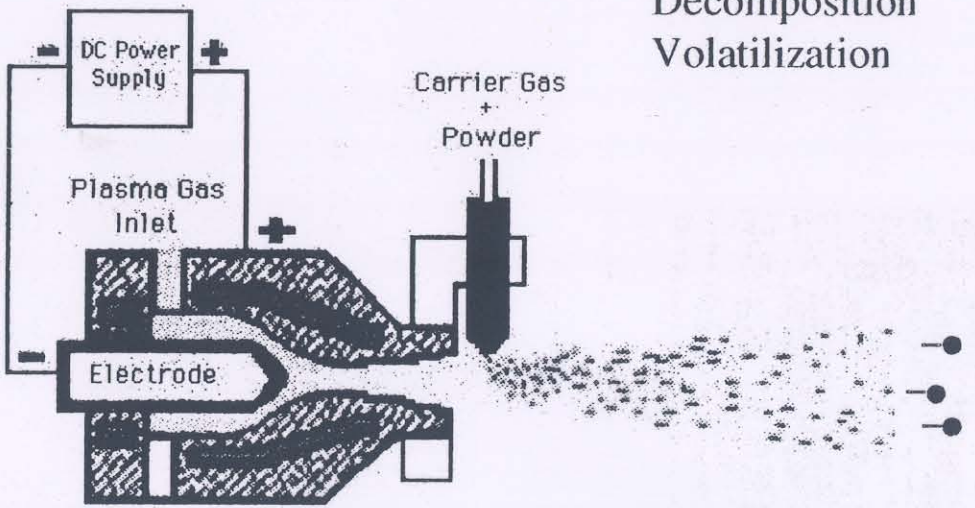

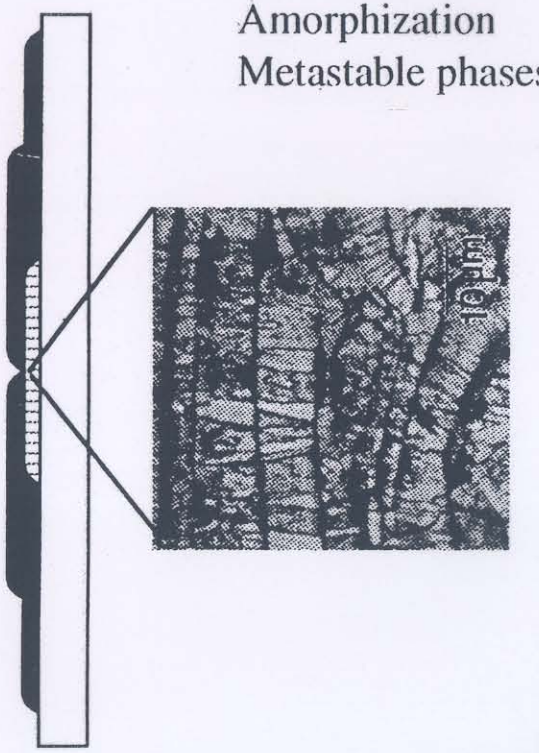

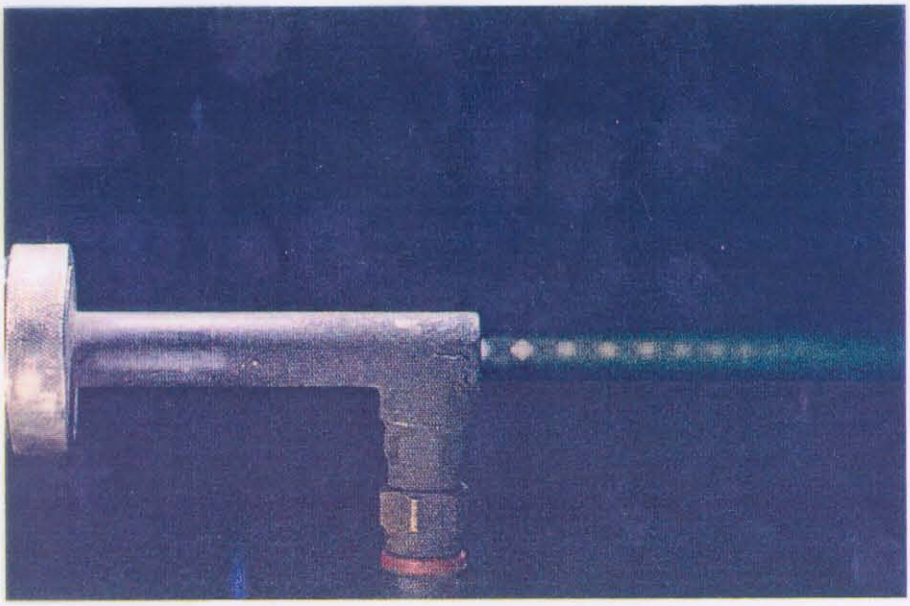

HVOF

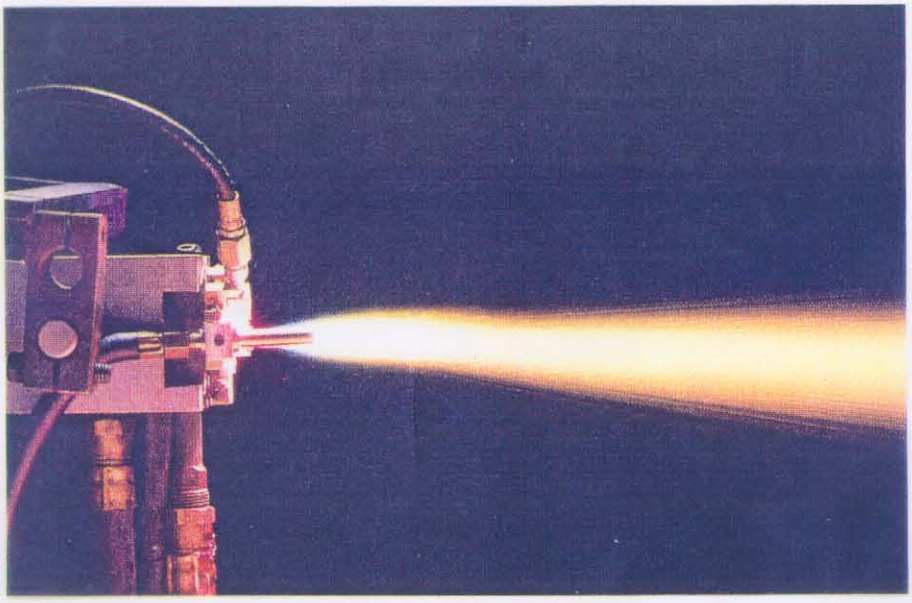

PLASMA

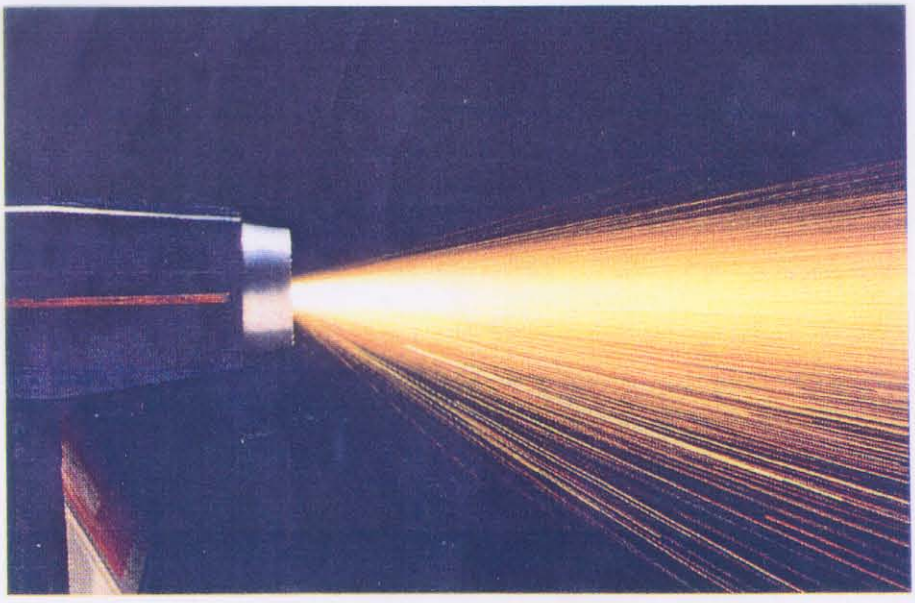

TWIN
WIRE ARC

Basic concepts used for powder injection in a plasma flow

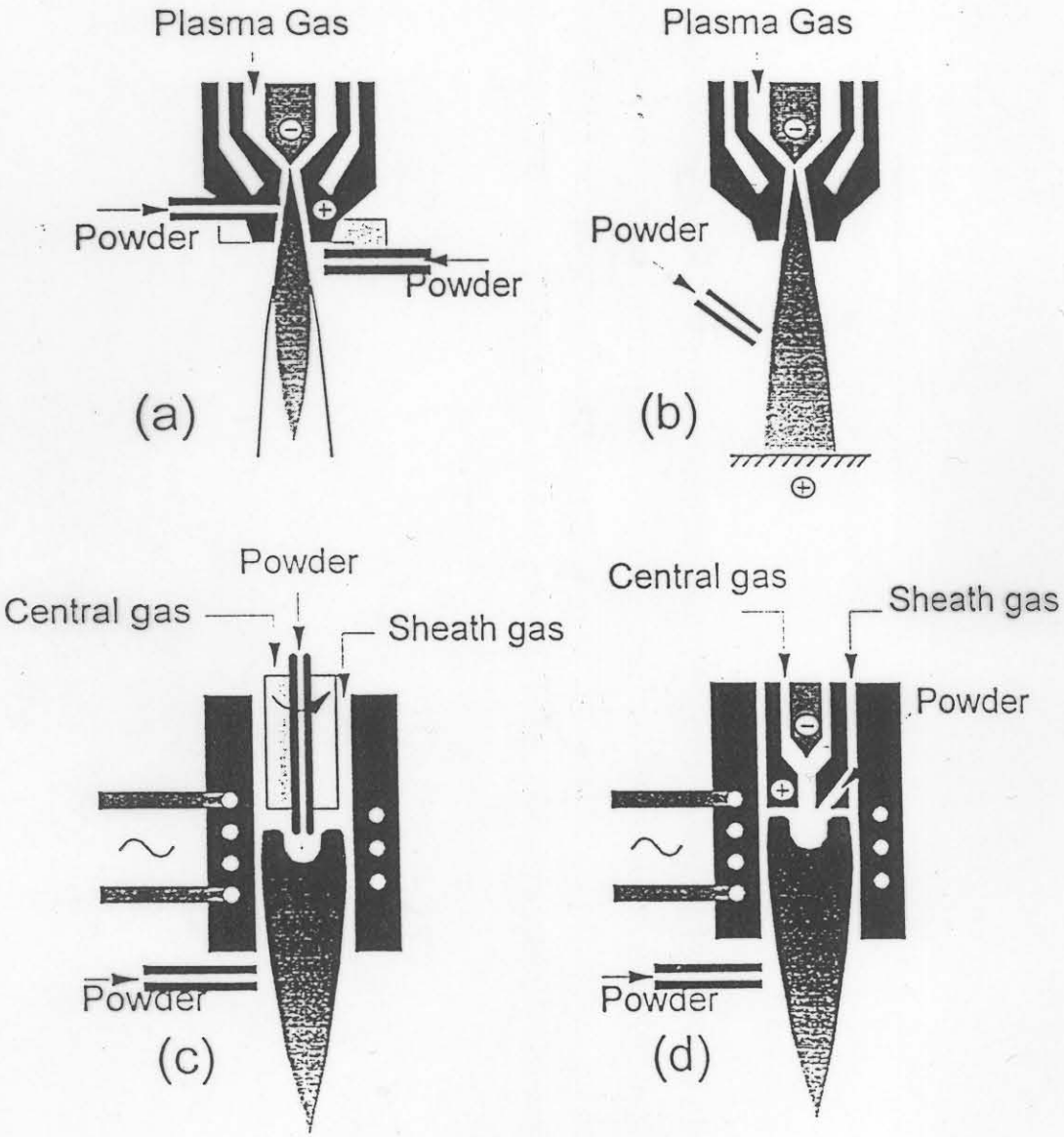

Flow field around a single sphere

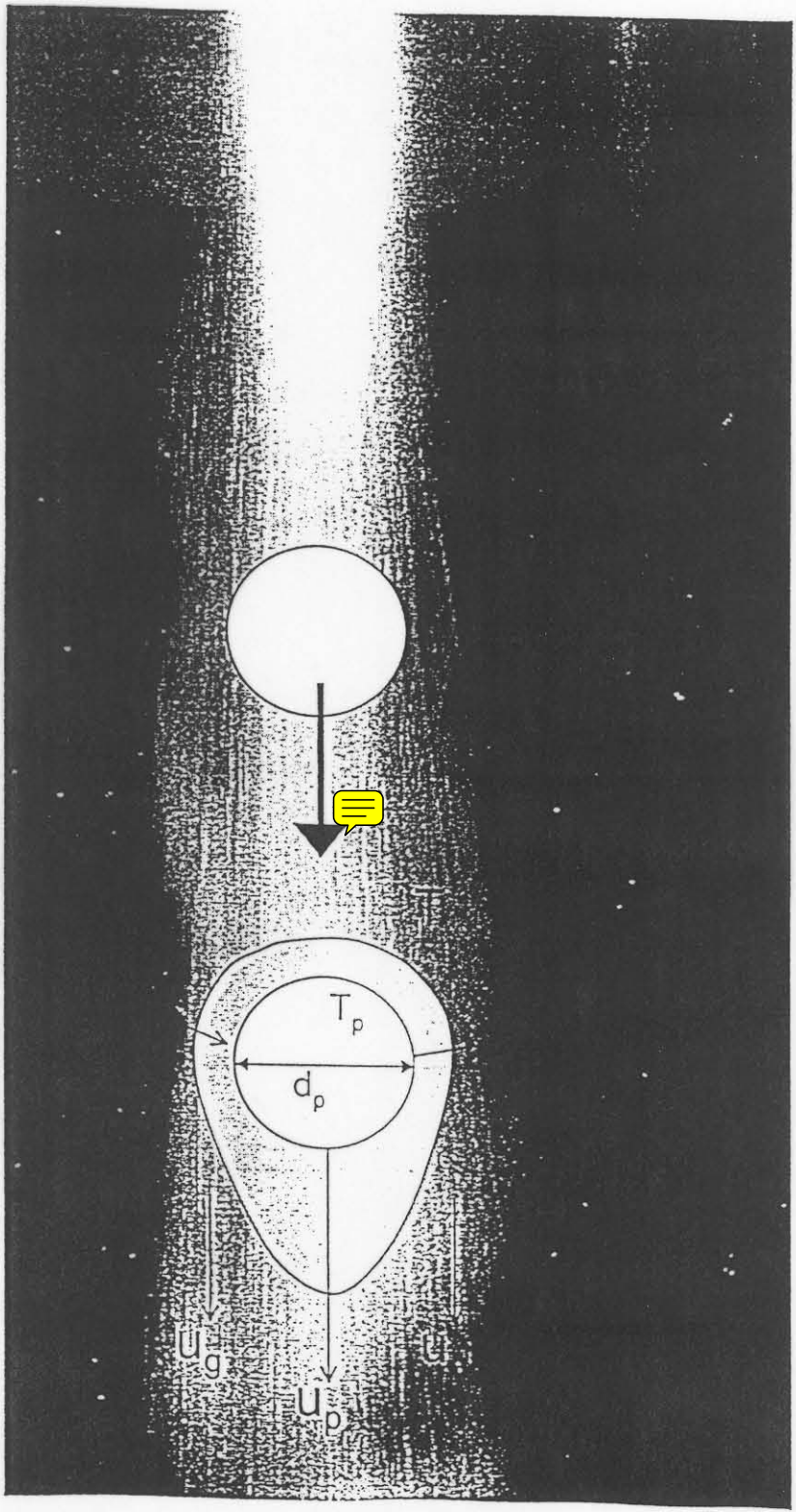

PLASMA - PARTICLE INTERACTION

Problem of the trajectory of a particle in the plasma stream

Important is the **temperature and the residence time**

= melting of the particle

= chemical and phase changes („burnout“, evaporation, ...)

PARTICLE - SUBSTRATE INTERACTION

Particle energy consists of thermal and kinetic energy

When falling at the substrate the particle deforms and forms so called **splat**

Originate two types of pressure:

1. **impulse pressure** (up to 1 GPa, duration 10^{-10} - 10^{-7} s)
2. **dynamic pressure** (50-100 MPa, duration 10^{-7} - 10^{-5} s)

- the splat form depends on the parameters of flying particle
- the heat exchange = amorphous layer induces columnar structure of the coating

When the melted particle falls at the substrate its energy changes to thermal and deformation energy. Part of the heat is transferred to the substrate at the impact position, the particle quickly cools down and solidifies. The deformation energy induces the change of the particle form into a flat disc as well as the pressure wave on the substrate surface. Originate impulse and dynamic pressure.

The impulse pressure reaches up to 1 GPa, but since its duration is very small ($t \sim 10^{-10}$ - 10^{-7} s) it does not influence substantially the mutual interaction between the droplet and the substrate. In influences positively, however, the destruction of oxide films on the substrate surface. The maximal value of the impulse pressure is given by the relation:

$p_i = \mu/2 \,.\, \varphi \,.\, c_{sound} \,.\, v_p$, where

p_i is the impulse pressure,
μ is the coefficient of the particle rigidity ($\mu \approx 0.5$),
φ is the density of the melted particle,
c_{sound} is the sound velocity in the melted particle material and
v_p is the particle velocity at the moment of the impact at the substrate.

Even if the **dynamic pressure** reaches much lower values, approximately 50-100 MPa, it is acting for much longer time, during 10^{-5}-10^{-7} s, and hence it has greater effect for reaching the optimum contact between the particle and the substrate. The magnitude of the dynamic pressure is given by the relation:

$p_a = \varphi \cdot v_p^2$, where

p_a is the dynamic pressure,
φ is the density of the melted particle and
v_p is the particle velocity at the moment of the impact at the substrate

Reference: Matějka, D, Benko, B., Plazmové striekanie kovových a keramických práškov, Bratislava, Alfa, 1988.

Conditions for creation of good quality coatings and free standing parts

Large number of parameters :

Plasmatron:

voltage, current density, construction of the stabilizing chamber, stabilizing medium, electrodes, ...

Powder and feeding method :

- chemical and physical properties of the powder used (melting temperature, phase composition, thermal conductivity, ...)
- size and form of the powder particles, carrier gas, ...
- throughput and speed of the powder feeding, ...

Substrate:

- state of the substrate surface (chemical cleanliness, roughness, ...), temperature,
- physical and chemical properties (thermal conductivity, thermal expansion coefficient, chemical activity, ...)

Arrangement of the spray gun:

- feeding and spraying distances, angle of spraying,
- number of feeding points, relative speed of the plasmatron, ...

Physical Issues in Thermal Spray Deposition

- **Splat Formation**
  - Splashing mechanisms
  - Splat parameters
- **Nucleation and Phase Selection**
  - Melt undercooling
  - Metastable phase
- **Crystal Growth Kinetics**
  - Solute trapping
- **Solidification Morphology and Microstructure Formation**
  - Planar vs Cellular
  - Transition of morphology

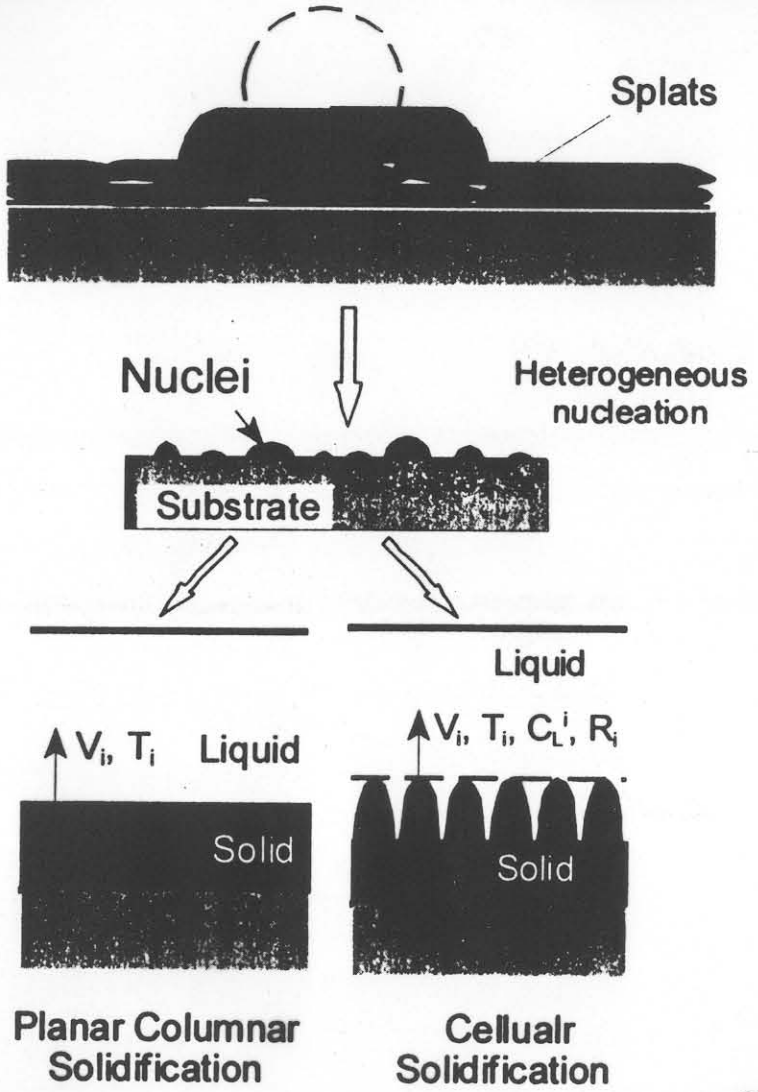

STONY BROOK

Internal stress can be divided into (i) structural and (ii) **thermal**

In the following consideration we shall treat **thermally** originated stress only.

Let us consider infinite flat interface without taking bending into account

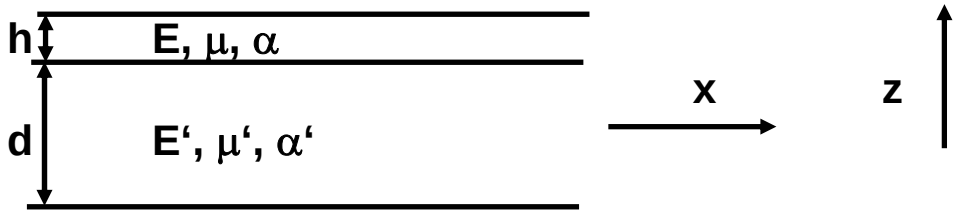

Upper layer material is characterized by E, μ, α, lower layer by E‘, μ‘, α‘.
(E-Elasticity modulus, μ-Poisson’s ratio, α-thermal expansion coefficient)
Upper layer is at temperature $\mathbf{T_1}$, lower layer at $\mathbf{T_1‘}$, and both temperatures relax to room temperature $\mathbf{T_0}$: $\mathbf{T_1 \rightarrow T_0}$, $\mathbf{T_1‘ \rightarrow T_0}$.

Let us assume that $\mathbf{T_1 \geq T_1‘}$ and $\mathbf{\alpha < \alpha‘}$. Then $\mathbf{\Delta T = T_0 - T_1 < 0}$ and $\mathbf{\Delta T‘ = T_0 - T_1‘ < 0}$.
Since the cross-sections are proportional to thicknesses, holds: $\mathbf{\sigma‘ = -\sigma . h/d}$ (σ is the stress). Since we assume **h<<d**, it is also $\mathbf{|\sigma‘| << |\sigma|}$. When the system cools down, there originates **elastic** deformation in the directions **x** and **y** (not **z**).

For the stress holds: $\sigma = \frac{\alpha' \Delta T' - \alpha \Delta T}{\frac{1-\mu}{E} + \frac{h}{d}\frac{(1-\mu')}{E'}}$.

For **h<<d** holds $\sigma \approx \frac{E}{1-\mu}(\alpha' \Delta T' - \alpha \Delta T) = Y(\alpha' \Delta T' - \alpha \Delta T)$ with **Y=E/(1-μ)**.

Special cases:
(i) **ΔT= ΔT‘** (hot substrate). Then **σ=Y(α‘-α)ΔT <0** results in **compressive** stress (coating **compresses** the substrate).
(ii) **ΔT‘=0** (cold substrate). Then **σ=-YαΔT >0** results in **tensile** stress (coating **stretches** the substrate).
For **ΔT‘/ΔT=α/α‘** results **σ=0** .
Condition **ΔT‘/ΔT>α/α‘** results in **compressive** stress.
Condition **ΔT‘/ΔT<α/α‘** results in **tensile** stress.

Example: sprayed **Al_2O_3 on steel**, **α≈8.10^{-6} K^{-1}, α‘≈12.10^{-6} K^{-1}, E≈280 GPa μ≈0.3**, **T_0=20 °C**, **Y=E/(1-μ)≈400 GPa, α/α‘≈0.66**.

For **T_1=1000 °C, T_1‘=800 °C: σ≈ -600 MPa - compressive** stress
For **T_1=1000 °C, T_1‘=200 °C: σ≈ +2270 MPa - tensile** stress
For **T_1=1000 °C, T_1‘=660 °C: σ≈ 0**

Poisson‘s ratio

When a sample of material is stretched in one direction it tends to get thinner in the other two directions.

Poisson's ratio is the **ratio of the** relative contraction strain, or **transverse strain normal to the applied load, to the** relative extension strain, or **axial strain in the direction of the applied load**.

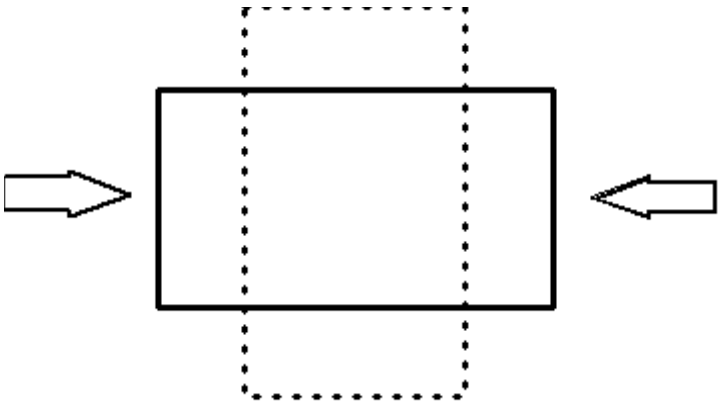

Poisson's ratio can be expressed as

$$\mu = - \varepsilon_t / \varepsilon_l$$

where

μ = *Poisson's ratio*

ε_t = *transverse strain*

ε_l = *longitudinal or axial strain*

Strain can be expressed as

$$\varepsilon = dl/L$$

where

dl = change in length

L = initial length

For most common materials the Poisson's ratio is in the range 0 - 0.5.

Typical Poisson's Ratios for some Common Materials

Material	Poisson's Ratio	Material	Poisson's Ratio
Upper limit	0.5	Polystyrene	0.34
Aluminum	0.334	Phosphor Bronze	0.359
Aluminum, 6061-T6	0.35	Rubber	0.48 - ~0.5
Aluminum, 2024-T4	0.32	Stainless Steel 18-8	0.305
Beryllium Copper	0.285	Steel, cast	0.265
Brass, 70-30	0.331	Steel, Cold-rolled	0.287
Brass, cast	0.357	Steel, high carbon	0.295
Bronze	0.14	Steel, mild	0.303
Concrete	0.2	Titanium (99.0 Ti)	0.32
Copper	0.355	Wrought iron	0.278
Cork	0	Z-nickel	0.36
Glass	0.24	Zinc	0.331
Glass, Ceramic	0.29	Nickel Silver	0.322
Ice	0.33	Nickel Steel	0.291
Inconel	0.27 - 0.38	Polystyrene	0.34
Iron, Cast - gray	0.211	Phosphor Bronze	0.359
Iron, Cast	0.22 - 0.30	Rubber	0.48 - ~0.5
Iron, Ductile	0.26 - 0.31	Stainless Steel 18-8	0.305
Iron, Malleable	0.271	Steel, cast	0.265
Lead	0.431	Steel, Cold-rolled	0.287
Magnesium	0.35	Steel, high carbon	0.295
Magnesium Alloy	0.281	Steel, mild	0.303
Molybdenum	0.307	Titanium (99.0 Ti)	0.32
Monel metal	0.315	Wrought iron	0.278
Nickel Silver	0.322	Z-nickel	0.36
Nickel Steel	0.291	Zinc	0.331

Physical mechanisms of adhesion

in the literature : Van der Waals force => NO!

- most often it is the mechanical wedging of the splat into the roughness of the surface => the rougher the surface the better adhesion
- additionally also the (diffusion) chemical bond can contribute to the coating adhesion

Comment to the chemical bond:

Experiment with Mo drop

- usually
  - the fresher the surface (after cleaning, sand blasting, ball burnishing etc.) the better adhesion
  - the higher substrate temperature the better adhesion
- possibility of exothermic reaction (on Al based substrates)
- problem of detection of local bonding

Structure of the sprayed coating

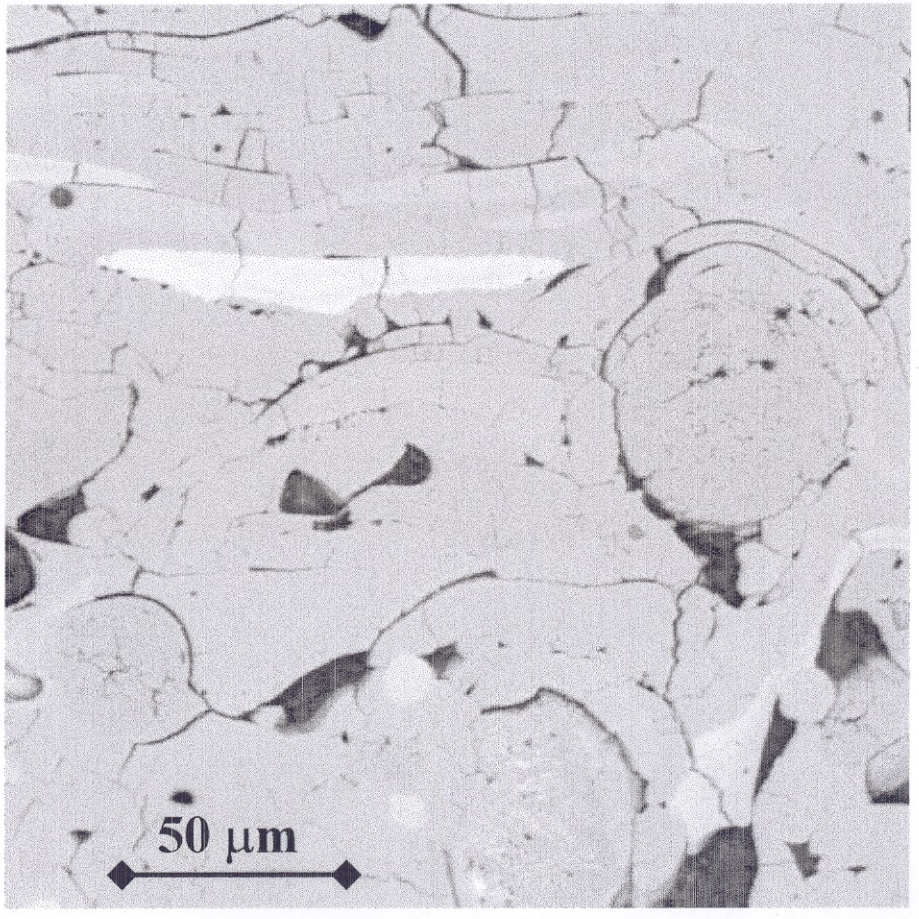

Cross-section, SEM

- rough, spherically shaped particles that solidified before the impact

- pores
  (i) spatial (three-dimensional)
  (ii) surface pores (two-dimesional)
    - in between splats
    - inside the splats

PORE SIZE DISTRIBUTION COMPARISON

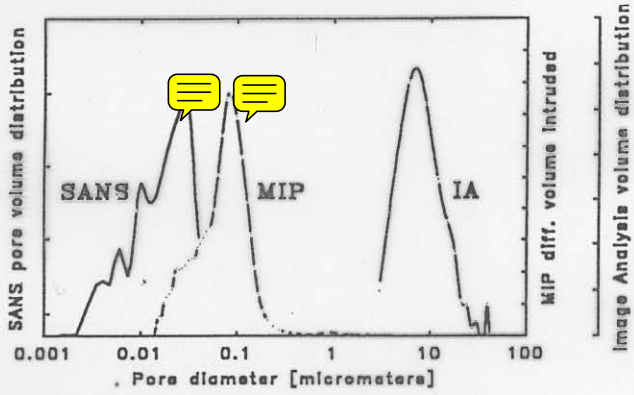

- PLASMA SPRAYED ALUMINA - AH
- MIP, IA & ARCHIMEDEAN POROSITY AROUND 6-7%
- DIFFERENT DISTRIBUTION FROM EVERY TECHNIQUE

METHODS COMPARISON

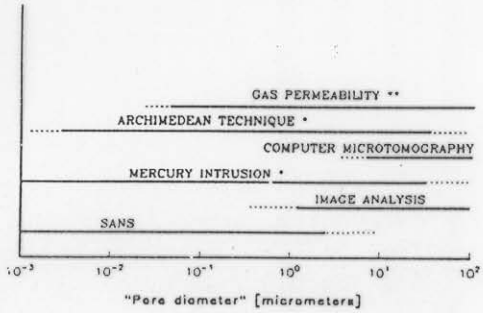

PORE SIZES MEASURED BY DIFFERENT TECHNIQUES

* OPEN PORES

** THROUGH PORES

Small Angle Neutron Scattering

- **The technique of small-angle neutron scattering (SANS) is used for studying the structure of a material on length scale of 10 to 1000 Å. In particular, SANS is used to study the shapes and sizes of the particles/pores dispersed in homogeneous medium.**
- **It involves scattering of a monochromatic beam of neutrons from the sample and measuring the scattered neutron intensity as a function of the scattering angle.**
- **Neutrons are not electrically charged with magnetic spin ½. Typical wavelength = 2 Å and energy available at most reactors is 0.1 – 500 MeV.**
- **Small scattering angles (~ 0.5–10°).**
- **Neutrons can penetrate a sample far better than other scattering techniques. This is because neutrons are electrically neutral.**
- **Two types of neutron scattering: Scattering due to nuclear interaction and a magnetic interaction due to unpaired electron.**

Principle of SANS

- **Monochromator (filters neutrons at different wavelenghts), collimator (slit used to sample beam size), sample table (10X10cm), 2-D detector.**

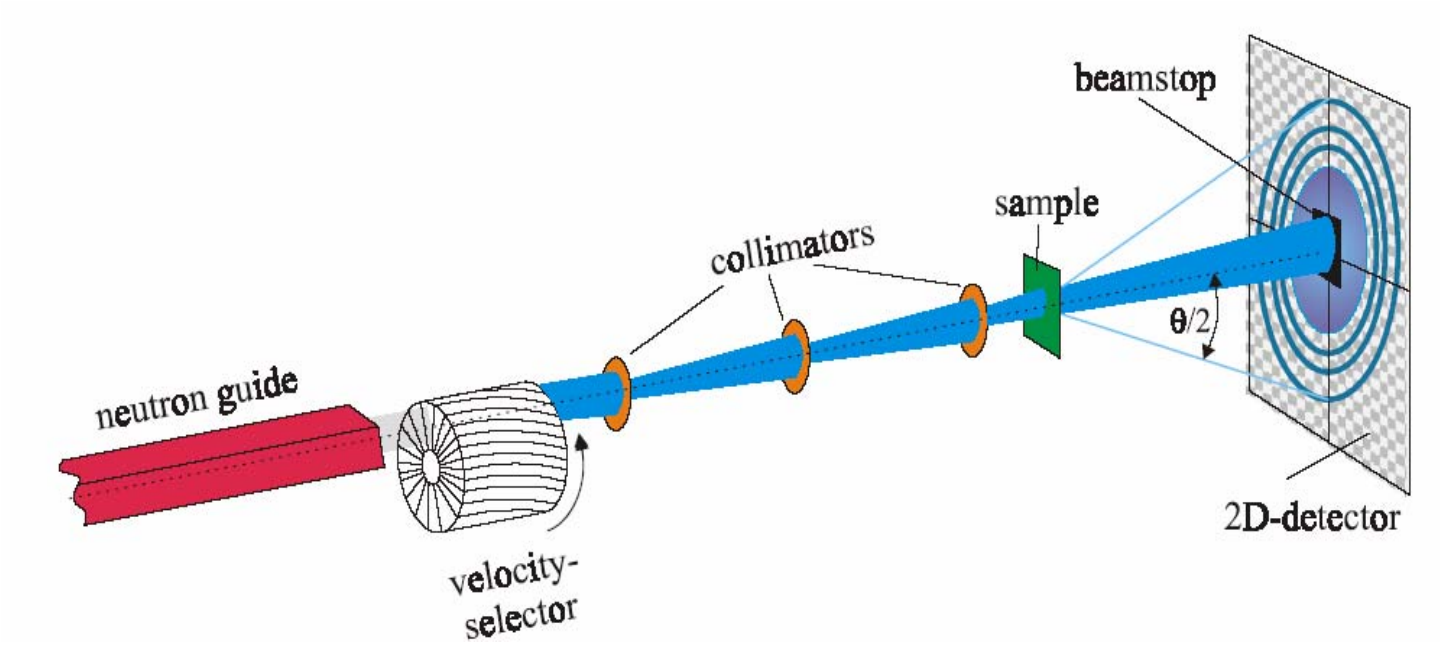

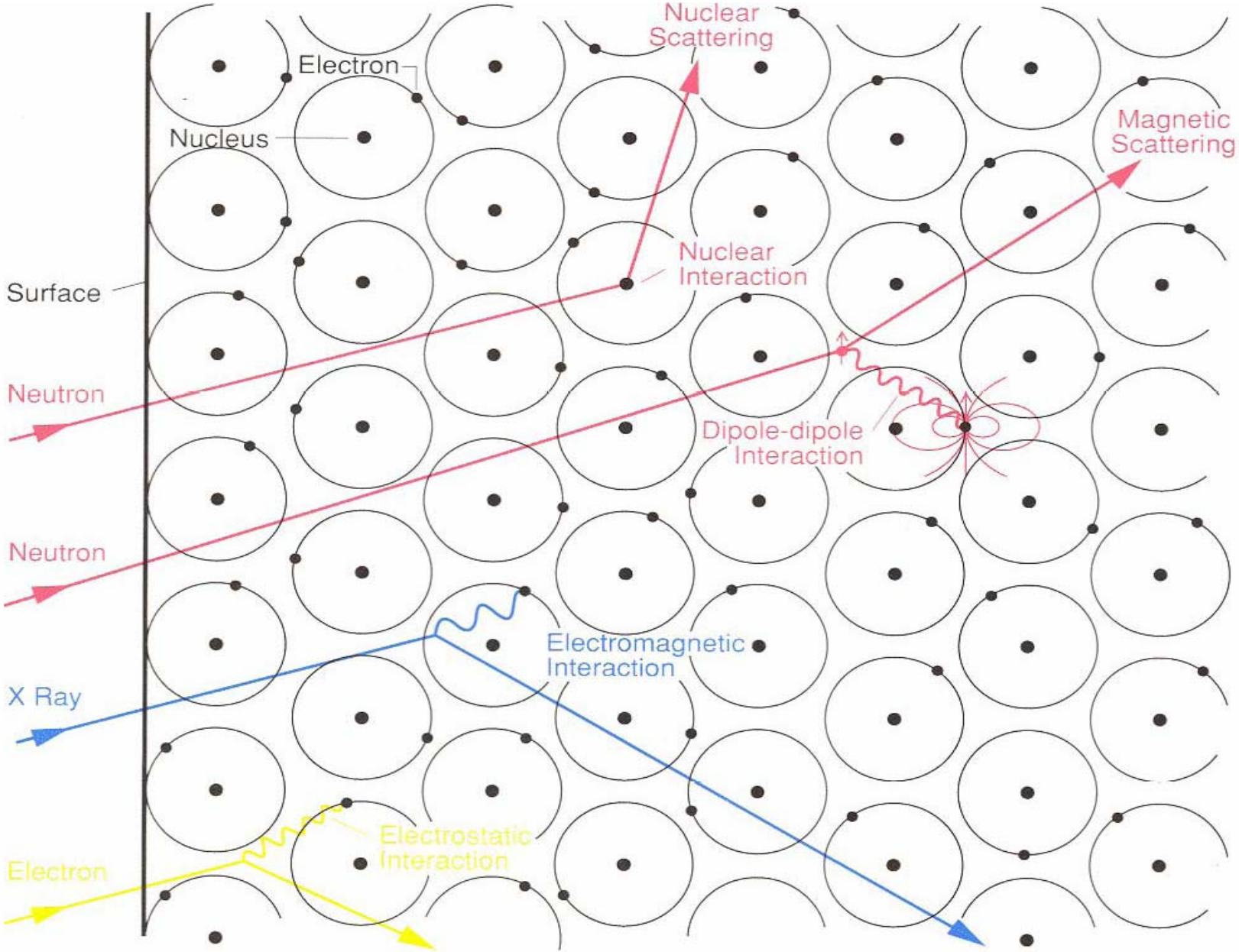
Nuclear Scattering
Electron
Nucleus
Magnetic Scattering
Nuclear Interaction
Surface
Neutron
Dipole-dipole Interaction
Neutron
Electromagnetic Interaction
X Ray
Electrostatic Interaction
Electron

30m NIST SANS

Mercury Intrusion Porosimetry

General

Mercury Intrusion Porosimetry (MIP) is a technique used to measure pore size distribution, and has an advantage in that it is able to span the measurement of pore sizes ranging from a few nanometres, to several hundred micrometers. Few other techniques exist that are able to measure the same range of pore sizes.

Theory

Mercury is a non-wetting liquid for almost all substances and consequently it has to be forced into the pores of these materials. Pore size and volume quantification are accomplished by submerging the sample under a confined quantity of mercury and then increasing the pressure of the mercury hydraulically. The detection of the free mercury diminution in the penetrometer is based on a capacitance system and is equal to that filling the pores. As the applied pressure is increased the radius of the pores which can be filled with mercury decreases and consequently the total amount of mercury intruded increases. The data obtained give the pore volume distribution directly and with the aid of a pore physical model, permit a simple calculation of the dimensional distribution of the pore size. Determination of the pore size by mercury penetration is based on the behaviour of non-wetting liquids in capillaries. A liquid cannot spontaneously enter a small pore which has a wetting angle of more than 90 degrees because of the surface tension (capillary depression), however this resistance may be overcome by exerting a certain external pressure. The pressure required is a function of the pore size, the relationship between pore size exerted when the pore is considered to be cylindrical, is expressed as:

$$pr = 2s\cos(q) \quad (1)$$

where r = pore radius.
s = surface tension of mercury.
q = contact angle (wetting angle).
p = absolute pressure exerted.

The relationship is commonly known as the Washburn* equation. Although in almost any porous substance there are no cylindrical pores, this equation is generally used to calculate a pore size distribution from mercury porosimetry data. The Washburn equation is derived from the following considerations: in a capillary with a circular section, the surface tension of the liquid is exerted in the area of contact over a length equal to the pore circumference. This force is perpendicular to the plane of the contact surface

The force tending to push the liquid out of the capillary is:

$$2\pi rs \cos q$$

Against this force, the external pressure will be exerted over the area within the contact circumference, equal to:

$$\pi r^2 p$$

When equilibrium is reached, these two forces have the same value:

$$2\pi rs \cos q = \pi r^2 p$$

Equation (1) therefore shows the pore radius is inversely proportional to the pressure:

$$r = 2s \cos q / p$$

When using mercury (taking the surface tension as 480 mN/m^2 and wetting angle as 141.3°) and assuming that all pores are cylindrical, the following relationship is obtained.

$$r = 7500/p \qquad (2)$$

where r is the pore radius in nm
p is absolute applied pressure in kg/sq.cm

For irregular shaped pores the ratio between the pore cross-section (related to the pressure exerted) and the pore circumference (related to the surface tension) is not proportional to the radius and depending on the pore shape, equation (2) will give lower values. The wetting angle (taken as 141.3°) depends on the nature of the sample, and should therefore be considered as an average value only. Surface tension should also be considered as a variable value. At 25°C it is 484.2 dynes/cm^2, while at 50°C it is 472 dynes/cm^2 ; 480 dynes/cm^2 has been taken as an average value.

Specimens prepared for testing are dried to remove all moisture from the pore structure. They are then placed into sealed 'penetrometers' which are weighed both before and after being loaded with the specimen. The penetrometers are placed into the machine where they are evacuated and then filled with mercury. The pressurized testing then commences and the machine calculates and records how much mercury is being forced into the pore structure based on the above equations.

* **Washburn, E.W.** (1921) A method of determining the distribution of pore sizes in a porous material. Proceedings of the National Academy of Sciences **V.7** (115).

The results obtained from the instrument are:

- pore size distribution (macro/meso range of porosity spectrum)
- hysteresis curve
- specific surface
- bulk density
- total porosity (%)
- particle size distribution

Normally these data are transferred into a spreadsheet or similar application for further detailed analysis.

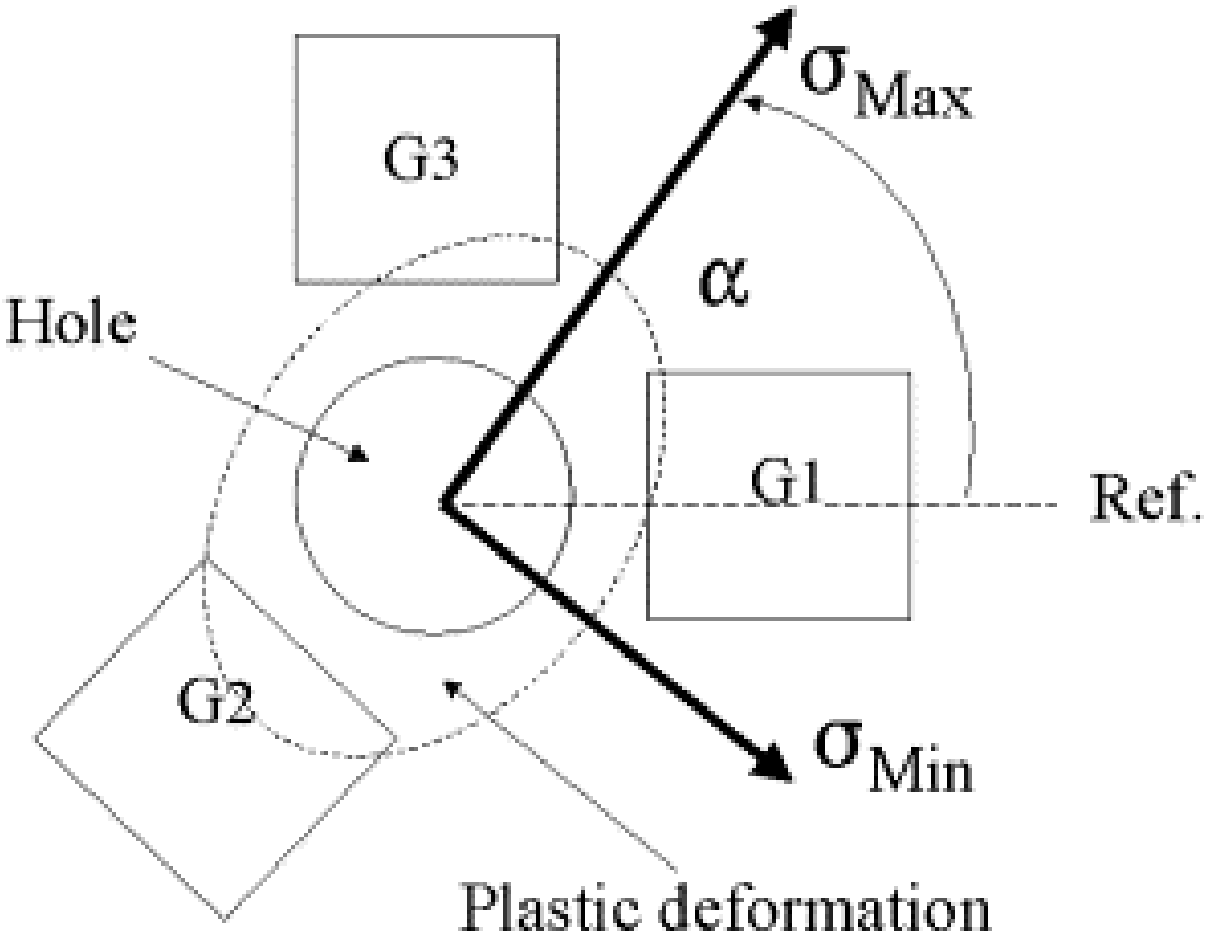

Strain gauge layout and directions of the principal stress components oriented with respect to a chosen laboratory direction reference.

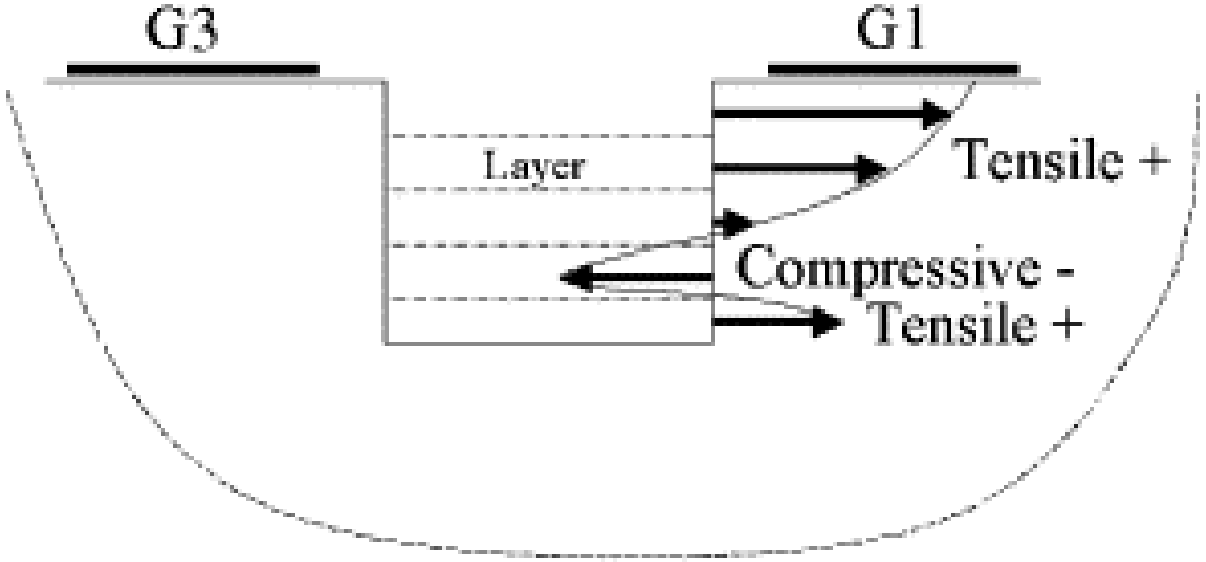

Cross section of the hole drilling location with the varying residual stress marked with arrows denoting tensile and compressive amplitudes in imaginary layers h_i.

Assessment of the coating homogeneity

<u>oversprays:</u> individual particles
inner homogeneity - „microhomogeneity

<u>sprays:</u> massive coating
„macrohomogeneity“ and „microhomogeneity“

<u>Some observed changes during plasma spraying:</u>

- **burn-out or evaporation of phases:** Na_2O, TiO_2, SiO_2
- **oxidation:** AlNi, metals in general
- **phase changes:** also in dependence on the speed of cooling
- **contaminants:** impurities

Chemical Homogeneity Measurements

(step by step quantitative analysis by XMA)

Micro-homogeneity: inside of a splat or a free-flight particle

Macro- homogeneity: over deposit

Homogeneity coefficient H:

$$H = (C_{max} - C_{min}) \times (C_{mean})^{-1/2}$$

where:

C_{max} , C_{min} and C_{mean} represent the maximal, minimal and mean concentrations of minor elements

10 – Plasma spraying
10.10. Coating generation – Example of results

1/ ZrO_2-Y_2O_3 (8% wt) influence of powder morphology and size

Main types of powders available

- Fused and crushed : blocky and angular, phase : c, dense alloyed ; $\rho \sim 6{,}000$ kg/m^3

- Agglomerated : almost spherical, porous, phase : m alloyed (heterogen, grain sizes 1-5 μm) $\rho \sim 3{,}400$ kg/m^3

- Agglomerated and sintered : blocky - angular, dense - porous, phase : c + t, alloyed, $\rho \sim 5{,}800$ kg/m^3

- Zyrcit : sol-gel-agglomerated - densified : almost spherical, porous, phase : m, alloyed (heterogen, grain sizes ~ 0.1 μm) $\rho = 4000$ kg/m^3

Phase symbols : c = cubic, m = monoclinic, t = tetragonal

PEROVSKITE STRUCTURE

Perovskites are materials the crystalline buildup of which is characterized by cation cubical main lattice consisting of an element of transitional metals group and by octaedric sub-lattice consisting of oxygen, in which the interstitial nodal point are occupied by cation of an other element.
Formal record: ABO3

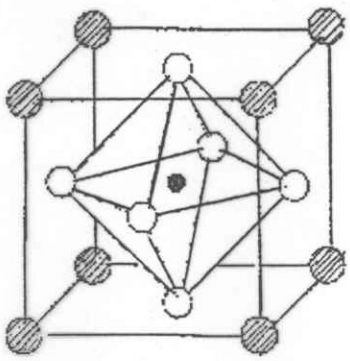

A ● B ○ O

$8 \times \frac{1}{8}$ A
1×1 B
$6 \times \frac{1}{2}$ O

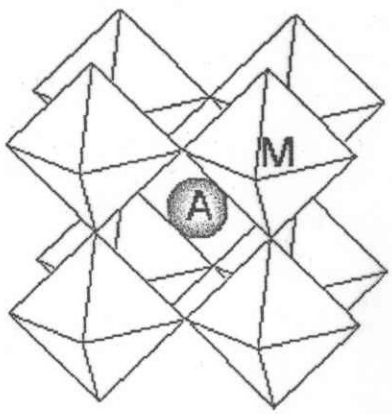

M - octaedric sub-lattice

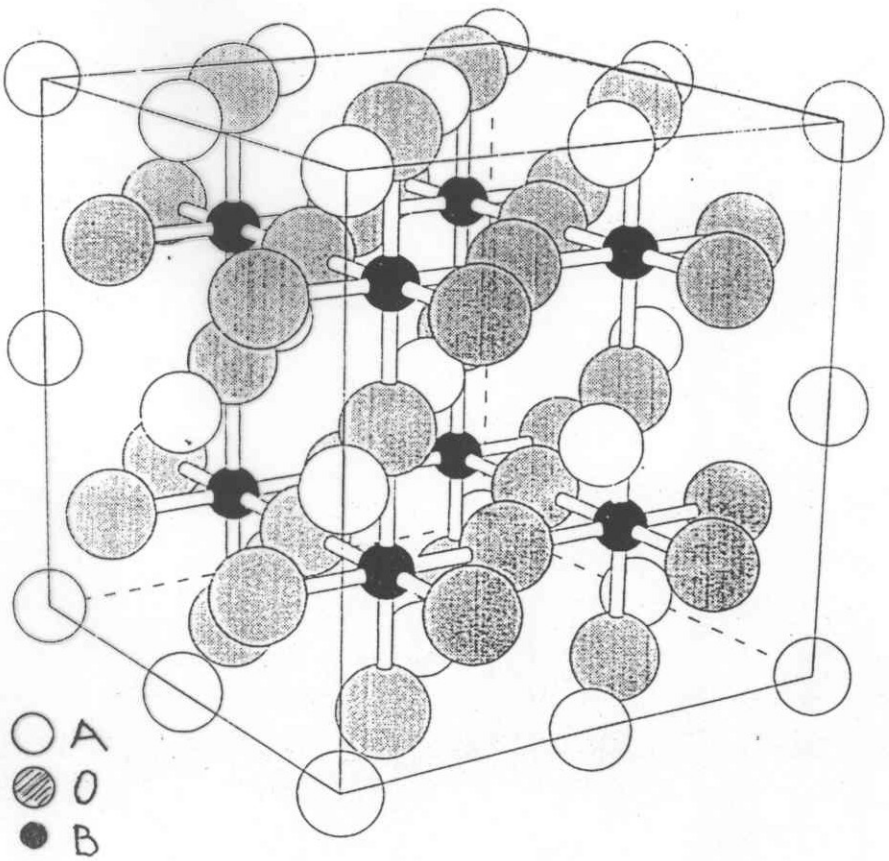

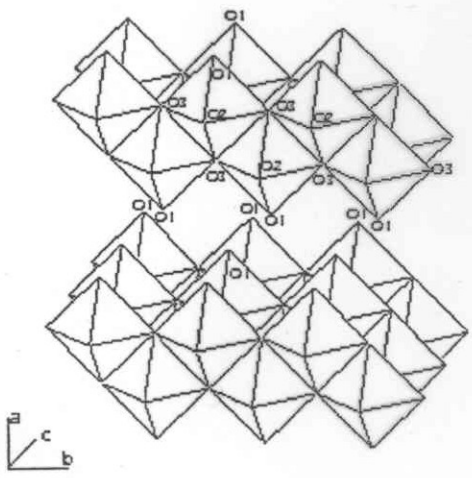

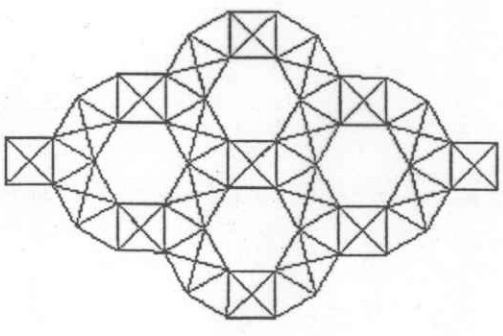

Cordierite is oxide ceramics based on AL2O3, highly resistant to thermal shock, has a low thermal expansion, provides excellent insulation properties in high relative humidity conditions and is highly resistant to aggressive substances. Major industrial applications: power switch components, regulating rheostat components, catalyst substrates.

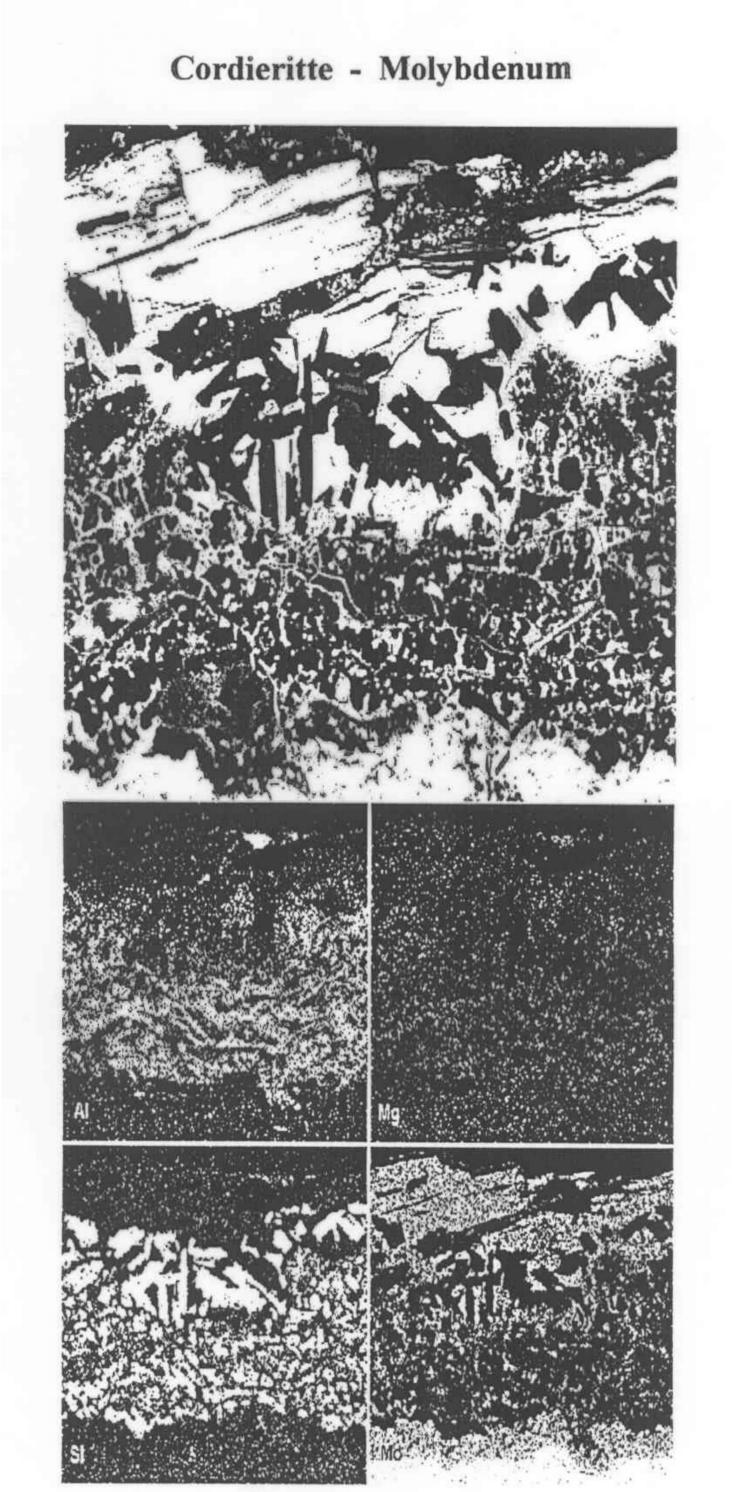

- two procedures of manufacturing free standing ceramic parts (FSP) by plasma spraying

(**1**) mandrel covered with a **soluble layer**
-> dissolved after spraying

(**2**) „playing“ with the **thermal expansion coefficients** of the mandrel and of the deposited material
(= generally used at IPP)

INSTITUTE OF PLASMA PHYSICS
ACADEMY OF SCIENCES OF CZECH REPUBLIC

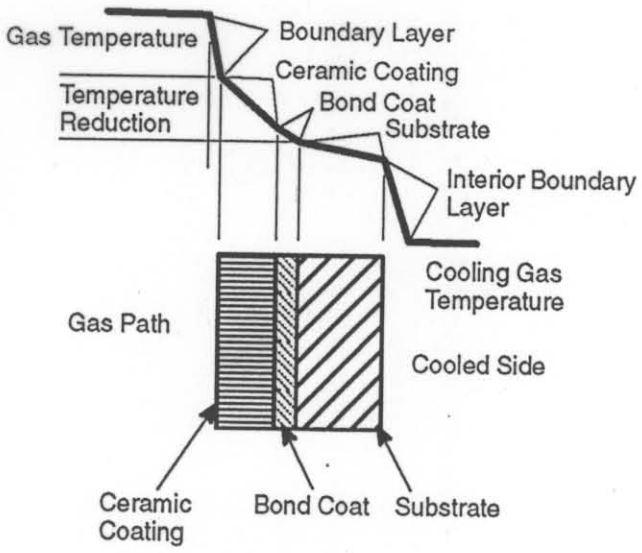

Fig. 1 Schematic of a thermal barrier coating

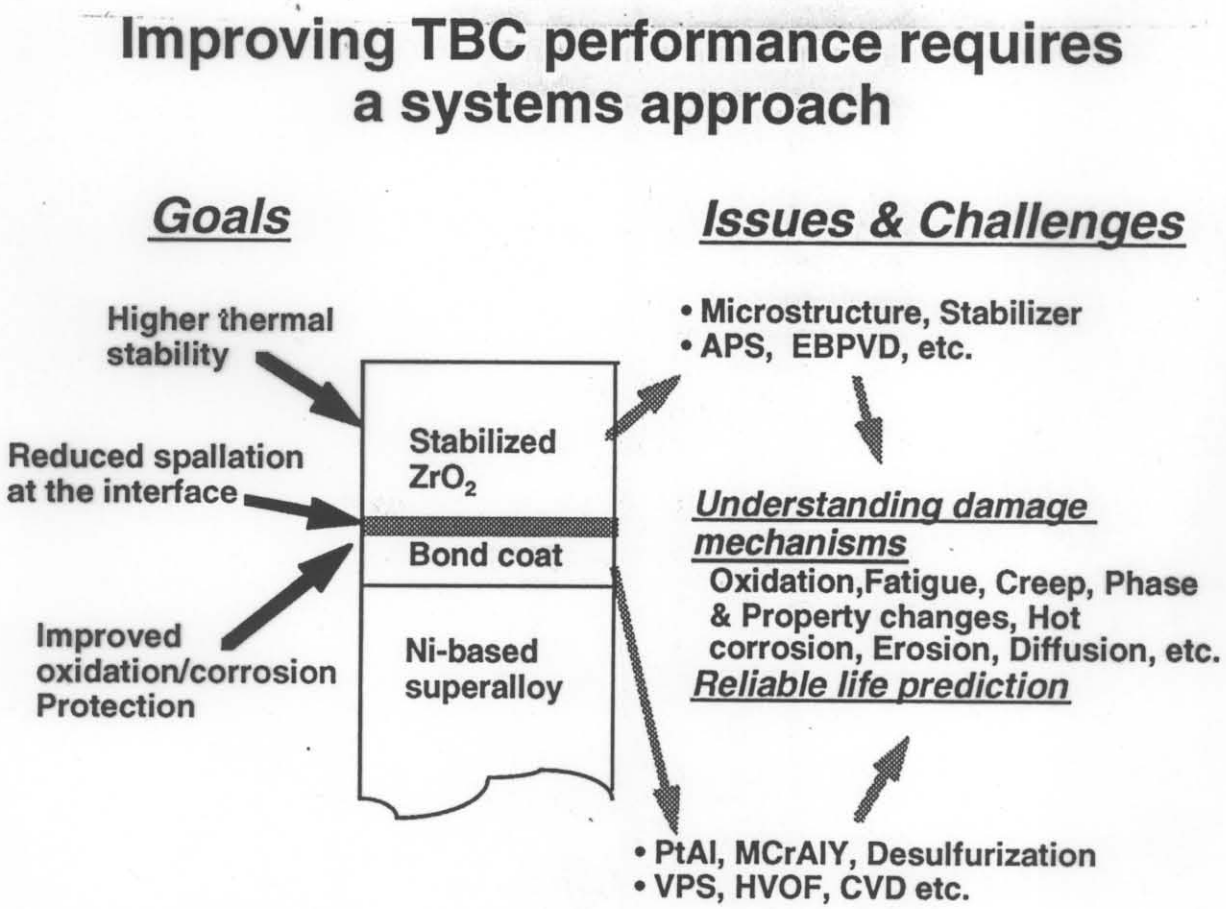

Fig. 3 Approaches for improving TBC performance

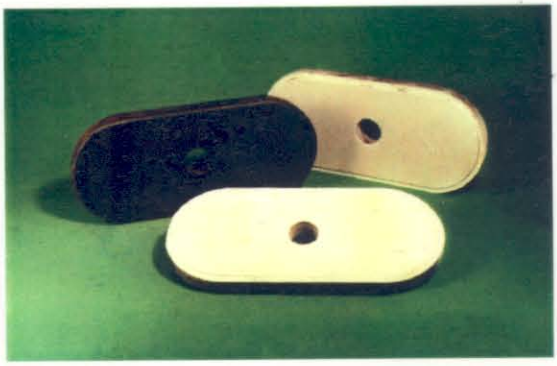

INSTITUTE OF PLASMA PHYSICS
ACADEMY OF SCIENCES OF CZECH REPUBLIC

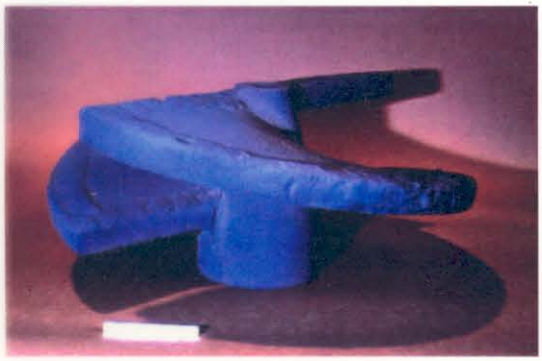

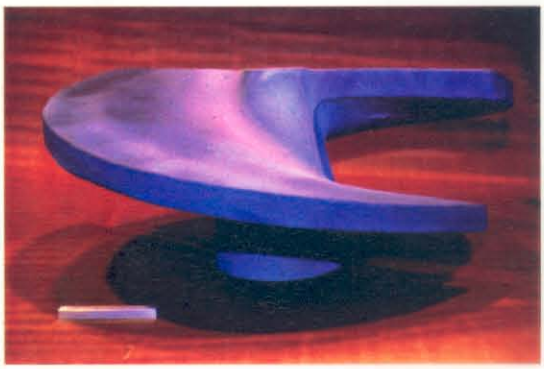

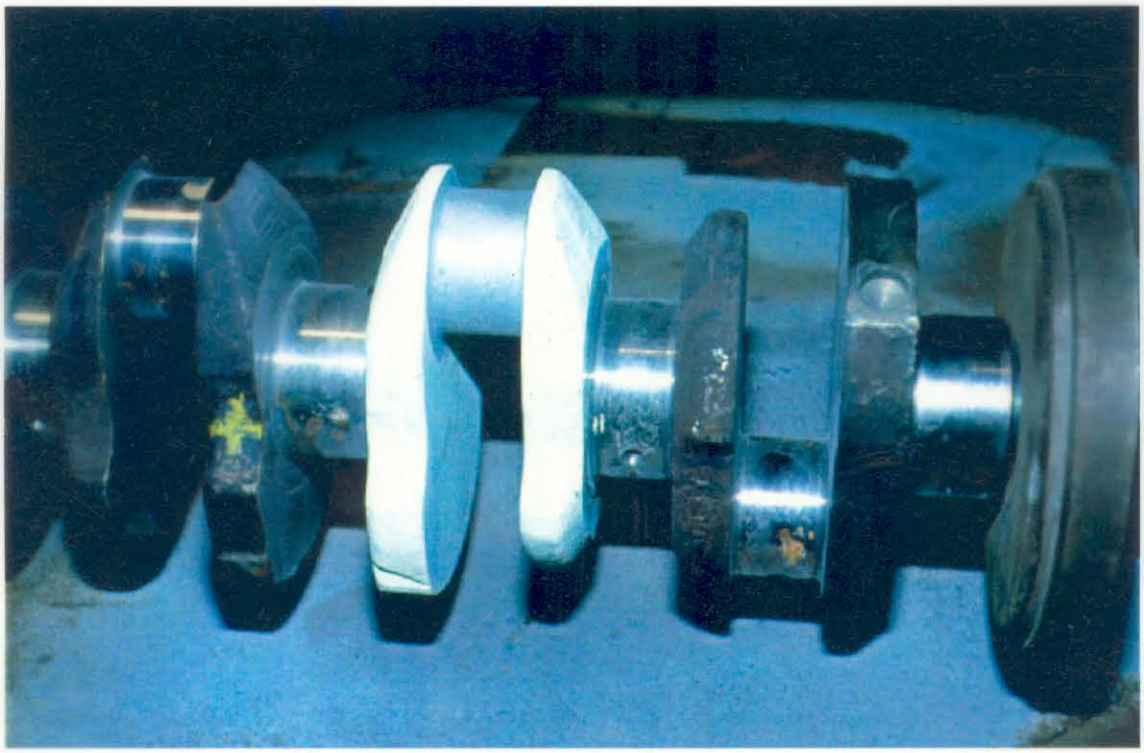

5. SELECTED EXAMPLES OF APPLICATIONS

WSP® 500

WATER STABILIZED PLASMA SPRAY SYSTEM

Applications

The WSP® 500 has a wide range of applications for use with a wide variety of materials, for example:

Print Industry
- **Print rolls**
- Analox rolls

Pulp & Paper Industry
- Calendar rolls
- **Granite rolls**
- Impellers and casings
- Refiner, Jordan and Clafin sleeves
- Rotors - Moyno rotors
- Yankee dryers

Petrochemical Industry
- Pump shafts, impellers, casings
- Pump sleeves
- Mechanical seal faces
- **Burners**

Aviation/Aerospace Industry
- **Engine parts**
- Combustion liners
- Rocket flare tubes
- Turbine castings

Oil Industry
- Pump plungers
- Compressor rods
- Mud pump shafts
- Pump sleeves

Textile Industry
- Draw rolls
- Thread guides
- Heater plates

Steel Industry
- Steel rolls, electrodes, lances
- **Hearth plates**
- Heart rolls
- Hot metal extrusion dies
- Graphite electrodes
- Oxygen lances
- **Fans**

- **Free-standing Ceramic Parts**

Glass and Ceramic Industry
- **Glass feeders**
- **Extrudes**

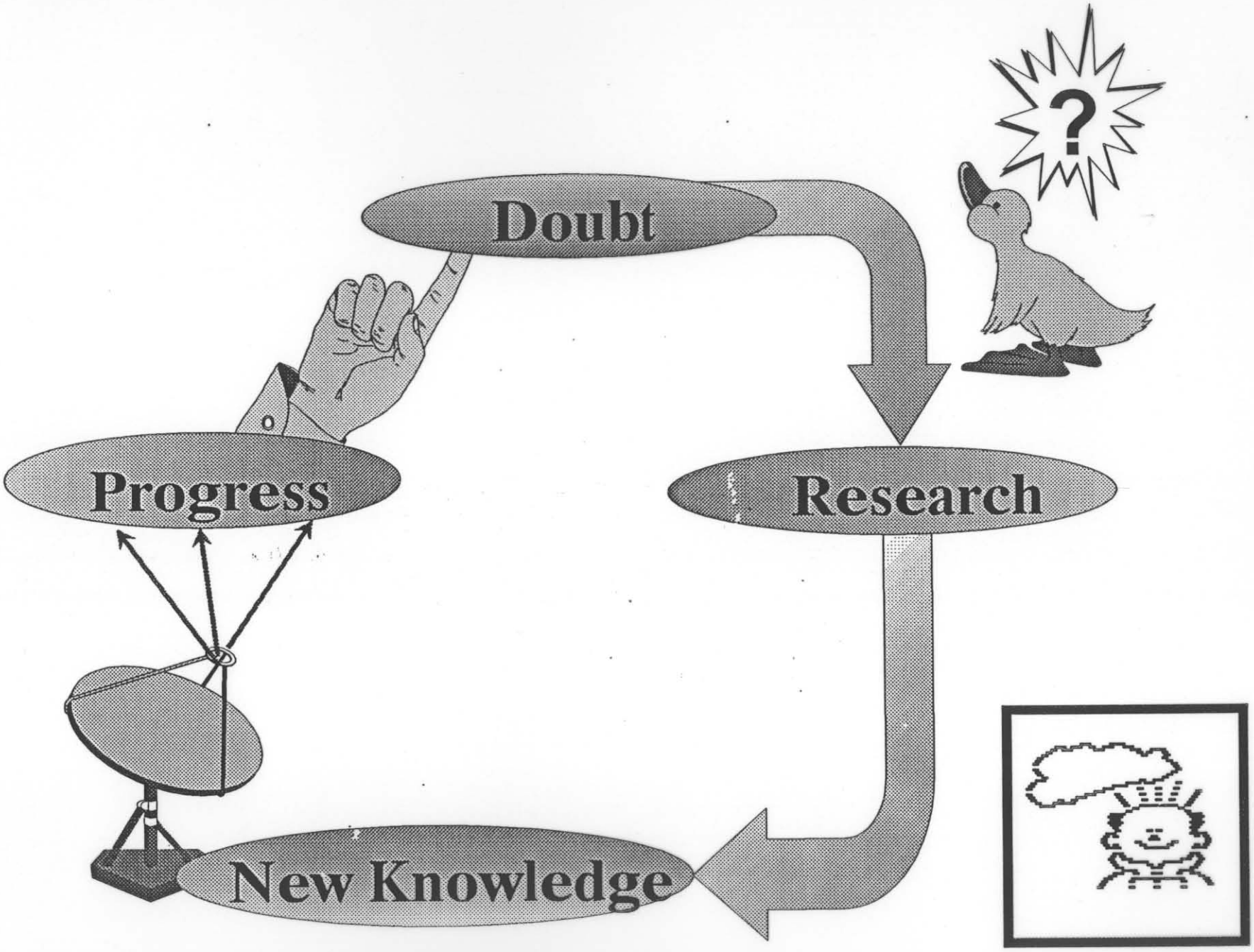
Doubt
Research
New Knowledge
Progress